Fly Ash Property Study

Laboratory Test Results

1000657

Fly Ash Property Study

Laboratory Test Results

1000657

Technology Review, December 2000

EPRI Project Manager

R. Altman

EPRI • 3412 Hillview Avenue, Palo Alto, California 94304 • PO Box 10412, Palo Alto, California 94303 • USA
800.313.3774 • 650.855.2121 • askepri@epri.com • www.epri.com

ORGANIZATION(S) THAT PREPARED THIS DOCUMENT

Southern Research Institute

This is an EPRI Level 2 report. A Level 2 report is intended as an informal report of continuing research, a meeting, or a topical study. It is not a final EPRI technical report.

ORDERING INFORMATION

Requests for copies of this report should be directed to the EPRI Distribution Center, 207 Coggins Drive, P.O. Box 23205, Pleasant Hill, CA 94523, (800) 313-3774.

CITATIONS

This document was prepared by

Southern Research Institute
2000 Ninth Avenue South
P. O. Box 55305
Birmingham, AL 35205-5305

Principal Investigator

J. McCain,

This document describes research sponsored by EPRI.

The publication is a corporate document that should be cited in the literature in the following manner:

Fly Ash Property Study: Laboratory Test Results, EPRI, Palo Alto, CA: 2000. 1000657.

ABSTRACT

Electrical resistivity of fly ash is one of the critical properties required to make accurate predictions of ESP performance. Dr. Roy E. Bickelhaupt of Southern Research Institute developed a correlation relating the mineral composition of coal fly ash to its electrical resistivity in the late 1970s. Predictive software based on this correlation has been in general use for about twenty years. It is recognized, however, that the accuracy of the resistivity predictions made with the original correlation and its successors are sometimes marginal. The principle cause for the lack of accuracy is believed to be due to the limited number of ash samples and tests used to develop the correlation. Furthermore, there were only one or two ashes from blended coals in Dr. Bickelhaupt's original study, and it is not known if the correlations produce accurate results for these ashes.

The objective of this effort is to improve the accuracy of the resistivity predictions based on ash mineral composition data. The end products of the study will include a report summarizing the results of the tests, updated predictive correlations, and a computer algorithms that performs the resistivity calculations and will replace the existing algorithms in EPRI's ESPM and ESPERT computer programs. This interim report contains descriptions and results of laboratory tests to measure the chemical and physical properties of new coal and fly ash samples solicited for this study.

TABLE OF CONTENTS

1 INTRODUCTION

Background

Fuel flexibility is an important issue for most utilities because it can help them achieve two goals: 1) lowering SO_2 emissions by burning a low-sulfur coal and 2) lowering operating costs by burning a lower cost fuel. However, identifying acceptable alternative coal supplies can be difficult and usually involves time-consuming and costly test burns. EPRI and others have developed a number of analytical tools that can help reduce the costs and uncertainties associated with the fuel selection process. The impact of an alternative fuel on particulate emissions is one of those areas where EPRI tools can be helpful. ESPM, ESPert, and the Southern Research Institute Model of Electrostatic Precipitation can be used to predict the affect of a new coal supply on ESP performance if important properties of the ash produced by the coal are known or can be predicted.

Electrical resistivity of fly ash is one of the critical properties required to make accurate predictions of ESP performance. Dr. Roy E. Bickelhaupt of Southern Research Institute developed a correlation relating the mineral composition of coal fly ash to its electrical resistivity in the late 1970s. Predictive software based on this correlation has been in general use for about twenty years. It is recognized, however, that the accuracy of the resistivity predictions made with the original correlation and its successors are sometimes marginal. The principle cause for the lack of accuracy is believed to be due to the limited number of ash samples and tests used to develop the correlation. Furthermore, there were only one or two ashes from blended coals in Dr. Bickelhaupt's original study, and it is not known if the correlations produce accurate results for these ashes.

Objectives

The objective of the work is to improve the accuracy of the resistivity predictions based on ash mineral composition data. This objective is to be achieved by gathering fly ash and coal samples from utility power plants that volunteered to participate in this study, performing the necessary laboratory studies on these samples, and generating new correlations for predicting resistivity. Sixteen new ash samples, including at least five samples from blended coals, have undergone physical and chemical analyses in the course of this study. This second interim report describes the results of these tests. Future products of the study will include a report updating the predictive correlations, and a computer program that performs the resistivity calculations. The first interim report on this work was published in 1999 (1). It presented a detailed review of the original predictive correlations developed by Dr. Bickelhaupt and an extensive bibliography on fly ash resistivity.

Early Work on Predictive Resistivity Correlations

Dr. Roy Bickelhaupt's study of the electrical resistivity of coal fly ash began in the early 1970s. This work focused on the study of volume conduction and surface conduction in fly ash. Test data indicated that for fly ashes consisting principally of a glassy phase, the volume conduction process was similar to that of common glass. It was determined that conduction occurs by an ionic mechanism in which the alkali metal ions serve as charge carriers (in the absence of sulfuric acid vapor). His research showed that the electrical resistivity was inversely proportional to the combined molecular concentration of lithium and sodium (2). Dr. Bickelhaupt conducted additional experiments demonstrating that surface conduction takes place by an ionic mechanism in which the alkali metal ions serve as the principal charge carriers. It was observed that the surface resistivity was inversely proportional to the concentration of these alkali metal ions (in the absence of sulfuric acid vapor). Previously, it had been generally accepted that surface conduction occurred by an electrolytic or ionic mechanism dependent principally on the physical and chemical adsorption of certain species on the ash surface to produce a conducting film. Dr. Bickelhaupt's research showed that the role of the environment is no less important in that these factors control the release of the alkali metal ions (3).

The results of Dr. Bickelhaupt's research on surface and volume conduction mechanisms provided the basic tools for developing a method for predicting fly ash resistivity based on the chemical composition of the ashes. To provide a complete set of data for developing these correlations, an exhaustive study of 35 coal fly ashes was conducted in the late 1970s. From this group, sixteen ashes were selected to investigate the effect of the variation in flue gas moisture concentration and ash layer electric field strength on resistivity. Eight of these ashes were further utilized in experiments to determine the effect of sulfur trioxide on resistivity. By combining the expressions defining the effects of these three factors on resistivity with the basic expression for resistivity as a function of ash composition, correlations were developed to allow the prediction of fly ash resistivity as a function of temperature knowing the ash composition, water and sulfur trioxide concentrations, and the ash layer field strength. This work was published in 1979 (4).

The laboratory tests showed that resistivity was strongly correlated to the concentrations of lithium, sodium, iron, calcium, and magnesium in the ashes. Strong correlations were also shown with moisture levels and sulfur trioxide concentrations. Mathematical expressions were developed relating volume resistivity to ash composition and surface resistivity to temperature and water vapor concentration. These were combined as a sum of parallel resistances. A mathematical expression was developed relating acid resistivity to temperature and sulfur trioxide concentration. Using the expression for parallel resistances, the surface-volume resistivity expression was combined with the acid resistivity expression to form the final predictive relationship.

Refinements in the Original Model

The original model developed in 1979 was labeled Model 1. Between 1980 and 1985 laboratory data relevant to the resistivity prediction model were periodically obtained. Usually these data simply verified previous observations. However, a series of tests were conducted using fly ashes having high concentrations of calcium and magnesium that showed extra sensitivity to water vapor concentration with respect to resistivity. This deviation from the previous resistivity/water vapor correlation used in Model 1 was incorporated into the computer program. This new program was designated Model 1A (5).

In 1986 a new fly ash resistivity predictive tool was published, Model 2 (5). The reason for this new model was a better understanding of the influence of sulfur trioxide on resistivity and the dependence of its influence on the concentration of alkali metals in the ash. The scope of the work for developing the new model was an evaluation of the quantitative effect of air environments containing water and sulfuric acid on the resistivity of fly ash. Ten new ashes were thoroughly characterized both chemically and physically. The parameters investigated included fly ash composition, sulfuric acid concentration (1 ppm to 10 ppm), water concentration (5% and 10%), temperature (115^{o}C to 200^{o}C), and field strength intensity (2 kV/cm to 12 kV/cm). The principal type of experiment was the determination of resistivity at three temperatures for three concentrations of sulfuric acid vapor (1, 4, and 10 ppm).

In 1990 Dr. Bickelhaupt updated the program slightly to account for observations relative to the combined concentrations of magnesium and calcium. There are three criteria for the selection of the slope of the acid resistivity curve as a function of reciprocal absolute temperature. New data and observations made since Model 2 was published demonstrate that improved predictions occur when the concentration of magnesium plus calcium is 5.0% for the criteria listed. With this change, the model, now designated Model 2A (6), shows better agreement with observation, and it becomes somewhat more conservative.

Between 1980 and 1984 a new predictive tool was developed by Dr. Bickelhaupt for predicting the effective volume resistivity of sodium-depleted fly ash layers in hot-side electrostatic precipitators. At hot-side ESP operating conditions fly ash resistivity is not dependent on either water vapor concentration or sulfuric acid vapor concentration, but solely on electric field strength and temperature since volume conduction is the only means of charge transfer through the ash layer. To create his data set, eight fly ashes were evaluated by subjecting 0.5-cm layers to a continuously applied voltage gradient of 4 kV/cm for periods of time up to 35 days at a temperature of 350^{o}C (662^{o}F). Resistivity was determined at temperature before the test started and after the long period of applied voltage used to create the sodium-depleted condition. Sodium depletion was determined to have gone to completion when current measurements made at regular intervals did not change by more than 10% in a 100-hour period. The temperature was then reduced to 536^{o}F (280^{o}C) and current measurements were repeated. The voltage was then increased to electrical breakdown of the fly ash layer. This procedure was used to provide data to determine the effects of temperature, time (and therefore sodium depletion), and electric field strength on resistivity. The model developed from this study was designated as Model SD (7).

Purpose of This New Research Effort

Users of the several resistivity predictor models over the last twenty years have found Model 1 to be the most conservative, generally predicting the highest resistivity for normal ranges of ash constituent concentrations. It has been found, for all models, however, that even small changes in the concentrations of certain constituents, [Mg + Ca] for example, can result in large step changes in the predicted value of resistivity. The development of revisions in the model to eliminate or smooth these unrealistic changes in resistivity has been the primary goal of this effort. In addition, coal blending is very common in the utility industry today. The current models may or may not work well with these blends. Incorporating additional coal blends into the sample database was another goal of this revision effort.

Physical and chemical properties of sixteen new coal and fly ash samples were measured to expand the database upon which the next-generation resistivity model will be based. The next section (Section 2) provides a detailed description of the test procedures used to measure the ash properties. The test results and a brief review of the analytical findings are presented in the following section (Section 3). The final section (Section 4) discusses the results and their implications for development of a next-generation model.

2 DEVELOPMENT OF THE DATABASE

Several steps are involved in the process of developing a next-generation resistivity predictor model. These steps will insure that there is a substantial set of data (based on previously characterized fly ashes, as well as new ashes specifically requested for this study) upon which to base a revised model. These steps are briefly described below.

Ash Sample Solicitation

A solicitation for appropriate coal and ash samples was prepared. The goal of this effort was to acquire samples primarily from utilities using blended coals. The solicitation was distributed by EPRI to its member utilities. From the samples provided by cooperating utilities and organizations, a total of fifteen samples were selected for inclusion in the program. Data on a sixteenth new ash for which measurements had been made for a commercial client were also included in the data set with the permission of the client.

Laboratory Ash Studies

The following tests were conducted on the coal and fly ash samples submitted for this study.

- Descending-temperature ash resistivity measurements were conducted on each sample. These tests were performed generally in accordance with IEEE Standard 548-1984, "Criteria and Guidelines for the Laboratory Measurement and Reporting of Fly Ash Resistivity." However, these measurements were made with the same radial-electrode cell used for the sulfur trioxide conditioning tests rather than the parallel plate cell called for by IEEE Standard 548-1984.
- Fly ash resistivity was measured with sulfur trioxide vapor in the conditioning gas flowing through the resistivity apparatus. These measurements were made at two SO_3 concentrations, nominally 3 ppm and 10 ppm, over the range of temperatures used by Dr. Bickelhaupt during the development of his original model. The radial-electrode cell and associated equipment used for the resistivity tests in environments containing sulfuric acid vapor has been described in detail elsewhere (8).
- Fly ash density was measured using the helium pycnometer technique. The instrument used for this measurement is a Micromeritics Model 1302 Helium-Air Pycnometer.
- Fly ash particle size distributions were measured with a Microtrac X100 Particle Size Analyzer.
- Specific surface area measurements (surface area per gram of material) were made using the Brunaeur-Emmett-Teller (BET) technique. Ashes that exhibit relatively high specific surface

areas are usually highly cohesive and tend to be composed of particles with somewhat irregular surfaces.

- Fly ash mineral analyses were performed at Southern Research Institute with the data being reported as oxides in weight percent. In addition, soluble sulfate and loss on ignition values were determined for each ash.
- Coal and ash mineral analyses were performed at Southern Research Institute using the appropriate ASTM designated procedures. These analyses were made for “representative” samples of the blended coals, when available, or for the individual coals that made up the blend, if not.

The laboratory studies outlined above are very similar, for measurements of the same type, to those used by Dr. Bickelhaupt in preparing the data sets used to develop the original model. The principal differences between the original measurements and the current ones are the addition of the BET specific surface area measurements and the use of the Microtrac instrument for measurement of particle size distributions rather than the Bahco device used by Dr. Bickelhaupt. All of the laboratory data obtained for this model revision are presented in this report. For completeness, Dr. Bickelhaupt’s original data concerning the effect of sulfur trioxide vapor have been reproduced in this report, as well.

3
LABORATORY TEST RESULTS

Fly Ash Composition, Mass Median Particle Diameters, and Surface Area

Measurements were made on 15 ash samples, five of which were obtained from the SRI Coal Combustion Facility with the remainder being supplied by various utilities cooperating in the EPRI program. Ash composition was measured for the same eleven elements (Li, Na, K, Mg, Ca, Fe, Al, Si, Ti, P and S, as oxides) as was done in Roy Bickelhaupt's original resistivity model studies.

In addition to the 15 ash samples described above, an additional sample submitted for resistivity analysis by a client of SRI has been added because it, unlike the 15 EPRI samples, was an ash that was difficult to condition with SO_3. Two similar, difficult to condition, ashes were included in Bickelhaupt's earlier work. This new ash adds one further sample to that number, for a total of three difficult-to-condition ashes.

Table 3-1 and Table 3-2 present the chemical compositions of the ashes to be used in the development of the improved resistivity model. Table 3-1 contains the data for the new ashes that were obtained as part of this project while Table 3-2 reproduces the analyses from Dr. Bickelhaupt's original report (included here for completeness). These tables also provide the results of particle size measurements (in the form of Mass Median Diameter, or MMD) and specific surface areas from the BET measurements. The MMD and BET results in both tables were all obtained as part of the current contract.

Table 3-3 provides the results of mineral analyses of samples produced by laboratory ashing of coal samples corresponding to the fly ash samples in Table 3-1. With the exception of SO_3, the compositions found from the coal analyses closely match those of the corresponding fly ashes. However, SO_3 ran about six-fold higher in the analyses of the laboratory ashed coal than in the corresponding fly ashes. The latter difference indicates that when fly ash resistivity is to be predicted based on mineral analyses of laboratory ashed coal, the concentration of SO_3 found in the analysis should be reduced by a factor of six when the data are entered into the model.

Because the time interval between Dr. Bickelhaupt's original work and the current effort was so great (more than 20 years), some of his flyash samples were reanalyzed to verify that the two databases are compatible. The results of these analyses are provided in Table 3-4. Comparison of the recent results with those reported by Dr. Bickelhaupt indicated good agreement between the two.

Resistivity Measurements

Descending temperature resistivity curves and resistivity *versus* temperature at two vapor-phase concentrations of SO_3 were obtained in a simulated flue-gas atmosphere for each of the fifteen samples selected for inclusion in this study. In addition, data from one client ash sample has been included. In the latter case, data were obtained for the descending resistivity curve and only one vapor-phase SO_3 concentration. All measurements were made using the "Radial Electrode Resistivity Cell" depicted in Figure 3-1 (8). (The standard cell used in IEEE Standard 548-1984, "Criteria and Guidelines for the Laboratory Measurement and Reporting of Fly Ash Resistivity" is depicted in Figure 3-2 (9).) The results of these measurements are provided in tabular form in Appendix A and are shown graphically in Appendix B. Again, results from Dr. Bickelhaupt's original work are reproduced here for completeness.

In Dr. Bickelhaupt's original work the descending temperature resistivity curves without SO_3 predicted by the model compared quite favorably with the measured values. When the model was used to provide predicted resistivity curves for the sixteen ashes used in the current work this was not found to be the case. Figure 3-3 illustrates a typical example from the current samples for which the measured and predicted curves differ by roughly a factor of four. Discussions with Roy Bickelhaupt concerning the manner in which his data were obtained revealed that his measurements without SO_3 were made with the standard "disk" type resistivity cell while the measurements with SO_3 were made with the "radial" cell he developed for that purpose. On the other hand, all of the measurements to date with the new ashes were made with the "radial" cell. Thus it appears that there is a systematic difference between the results obtained with the two types of cells. One possible reason for such a difference may lie in the compaction of the ash that occurs in the standard "disk" cell when the disk is placed on the ash surface. Such compaction will not occur when the "radial" cell is used.

As noted above, Figure 3-1 shows an illustration of the "radial" test cell. The resistivity is measured in the annulus between the inner disk and the ring electrode which encircles it. Measurements with the standard "disk" cell (Figure 3-2) would be equivalent to measuring the resistivity between the inner disk and the base of the radial cell. Dr. Bickelhaupt made comparison measurements using the radial cell in the center disk/base configuration and found results comparable with those obtained with the standard cell. However, information (if it ever existed) regarding any comparisons between measurements made with the standard cell and the "radial" cell used in the radial mode could not be found. A limited number of such comparisons were subsequently made as part of this work to help resolve this question and the results from one such comparison are shown in Figure 3-4. As can be seen, a systematic difference does appear to exist between the results obtained with the two types of cells.

Table 3-1. Results of Mineral, Particle Size and BET Analyses of New Fly Ash Samples.

Sample Number		Composition by Weight Percentage													
Fly Ash	Corresponding Coal	Li_2O	Na_20	K_2O	MgO	CaO	Fe_2O_3	Al_2O_3	SiO_2	TiO_2	P_2O_5	SO_3	TOTAL	MMD	BET
9896-1-57	**9896-1-52**	0.02	1.70	0.52	4.40	27.90	9.90	19.30	27.40	2.60	1.10	3.10	97.94	7.6	1.22
9896-1-58	**9896-1-53**	0.02	1.50	0.90	4.50	22.00	9.60	20.80	34.50	2.40	0.93	2.20	99.35	9.6	1.28
9896-1-59	**9896-1-54**	0.03	1.40	1.20	3.70	17.90	9.20	23.40	39.90	2.40	0.77	2.80	102.7	12.8	1.11
9896-1-60	**9896-1-55**	0.03	1.10	1.70	2.70	11.40	9.50	21.80	43.90	2.70	0.49	2.40	97.72	18.	1.02
9896-1-61	**9896-1-56**	0.04	0.87	2.20	1.50	4.70	10.20	24.70	51.00	2.20	0.24	1.30	98.95	30.6	1.03
9896-1-67	**9896-1-2**	0.04	1.10	1.90	2.00	7.00	6.30	25.80	51.90	2.40	0.46	1.30	100.2	33.7	10.60
9896-1-68	**9896-1-12**	0.04	1.20	2.40	1.80	7.40	13.10	25.50	45.60	2.10	0.32	1.60	101.06	9.8	4.30
9896-1-69	**9896-1-71**	0.01	4.00	1.90	5.70	19.90	9.00	14.40	42.70	0.92	0.27	1.60	100.4	21.1	0.63
9896-1-70	**9896-1-62**	0.01	1.60	0.97	2.60	10.20	5.90	21.50	54.50	2.00	0.57	0.40	100.25	39.1	5.64
9896-1-121	**9896-1-126**	0.02	0.40	0.53	2.00	9.60	8.40	23.20	53.20	2.00	0.64	0.75	100.74	58.8	3.28
9896-1-122	**9896-1-85**	0.04	1.30	1.50	1.60	3.50	9.00	26.90	51.80	1.80	1.60	0.36	99.4	15.3	6.29
9896-1-123	**9896-1-128**	0.04	0.47	2.60	1.90	8.80	16.30	24.40	42.90	1.60	0.94	0.73	100.68	8.3	1.37
9896-1-124	**9896-1-129**	0.05	1.10	4.30	2.20	3.00	7.60	26.40	52.40	2.00	0.62	0.23	99.9	41.2	1.18
9896-1-130	**9896-1-22**	0.02	1.80	0.50	4.60	25.10	5.70	19.40	36.60	2.50	1.20	1.40	98.82	18.3	0.84
9896-1-133	**9896-1-132**	0.04	0.36	2.90	0.84	1.40	5.30	30.00	55.10	2.40	0.28	<0.08	98.62	35.5	1.62
D492A [a]		0.05	0.76	1.01	0.59	0.95	7.04	29.46	58.34	1.35	0.09	0.16	99.80	7.6	1.22
	Minimum	0.01	0.36	0.50	0.59	0.95	5.30	14.40	27.40	0.92	0.09	0.16			
	Maximum	0.05	4.00	4.30	5.70	27.90	16.30	30.00	58.34	2.70	1.60	3.10			

a. Fly ash analysis provided by supplier.

Table 3-2. Chemical Characterization of Ashes from Original Sulfur Trioxide Study by Dr. R. E. Bickelhaupt and Recent Particle Size and BET Results for Same.

	Composition by Weight Percentage												
Sample #	Li_2O	Na_20	K_2O	MgO	CaO	Fe_2O_3	Al_2O_3	SiO_2	TiO_2	P_2O_5	SO_3	MMD	BET
301	0.03	0.51	1.7	1.3	4.4	5	25.8	59	1.7	0.31	0.35	19.7	1.55
302	0.01	0.29	0.71	1.8	12.6	4.1	24.6	52.9	1	0.13	0.24	32.9	2.18
303	0.05	0.34	0.42	6.3	19.5	4.3	24.1	41.2	1.5	0.31	0.94	10.4	1.03
304	0.04	0.19	2.7	0.85	0.56	4.1	32.2	56.4	2.3	0.15	0.18	21.9	1.17
305	0.05	0.34	3.1	1.1	2.2	12.5	27.1	50.5	1.8	0.33	0.57	30.8	.92
306	0.03	0.46	2.4	0.91	3.8	21.4	20.7	46.9	1.5	0.29	1.2	24.6	1.9
307	0.01	2.8	0.62	1.1	12.8	4.1	25.6	50.4	0.84	0.19	0.41	28.2	1.02
308	0.02	1.8	0.32	6.2	30.9	5.5	19.8	30.8	1.7	1.1	4.1	3.12	1.44
311	0.1	0.54	2.4	1.2	2.1	8.1	30.8	51.6	2.1	0.51	0.33	30.6	1.77
312	0.07	0.2	0.76	1.7	7.9	3.9	32.8	48.7	2.3	0.98	0.53	NA	NA

Table 3-3. Results of Mineral Analyses of New Coal Samples.

Composition by Weight Percentage

Sample #	Li_2O	Na_20	K_2O	MgO	CaO	Fe_2O_3	Al_2O_3	SiO_2	TiO_2	P_2O_5	SO_3	TOTAL
9896-1-52	0.02	1.40	0.29	4.50	22.60	7.90	14.20	25.70	2.10	0.84	18.90	98.45
9896-1-53	0.02	1.10	0.91	3.20	14.50	8.60	16.60	33.10	2.00	0.66	17.70	98.39
9896-1-54	0.03	0.90	1.30	2.40	10.20	8.50	18.30	39.60	2.30	0.50	13.70	97.75
9896-1-55	0.03	0.80	1.80	1.80	6.10	13.60	21.60	43.70	2.20	0.34	9.10	101.05
9896-1-56	0.04	0.80	2.40	0.87	1.40	10.50	26.70	51.90	2.30	0.11	1.90	98.89
9896-1-2	0.05	0.93	2.00	1.80	6.30	10.20	23.20	44.70	1.60	0.33	8.60	99.71
9896-1-12	0.04	1.40	1.90	1.50	5.40	11.10	26.30	43.60	1.70	0.17	5.40	98.51
9896-1-71	0.02	3.00	1.80	4.80	16.80	8.20	12.60	37.40	0.60	0.11	14.60	99.93
9896-1-62	0.02	1.50	0.83	2.80	11.30	5.50	19.10	45.40	1.60	0.45	9.00	97.5
9896-1-126	0.03	0.38	0.61	2.10	8.60	7.60	23.30	46.00	1.60	0.91	8.40	99.53
9896-1-85	0.04	1.10	2.00	1.30	3.30	8.10	25.60	53.70	1.10	1.00	2.10	99.34
9896-1-128	0.04	0.48	2.70	1.80	8.10	16.00	22.00	40.10	1.20	0.67	8.80	101.89
9896-1-129	0.05	1.00	4.40	2.00	4.20	8.30	26.00	49.40	1.20	0.70	3.90	101.15
9896-1-22	0.01	1.40	0.50	3.70	20.90	5.00	16.60	34.20	1.70	0.84	13.20	98.05
9896-1-132	0.04	0.42	3.00	0.91	1.50	6.20	30.00	53.40	2.10	0.28	1.40	99.25

Table 3-4. Reanalysis of Selected Ashes from Original Sulfur Trioxide Study by Dr. R. E. Bickelhaupt and Client Ash D492A.

Composition by Weight Percentage

Sample #	Li_2O	Na_20	K_2O	MgO	CaO	Fe_2O_3	Al_2O_3	SiO_2	TiO_2	P_2O_5	SO_3
301	0.03	0.74	1.70	1.2	4.3	5.4	23.8	59.6	1.3	0.2	0.82
302	0.01	0.39	0.71	1.8	14.4	4.6	23.0	53.6	0.83	< 0.02	0.58
304	0.04	0.42	2.60	0.9	0.37	4.6	30.8	58.3	1.8	< 0.02	< 0.02
308	0.02	2.0	0.29	6.7	36.3	5.9	20.1	18.9	1.6	1.0	5.2
D492A	0.05	0.64	2.30	0.83	0.60	5.7	30.9	56.1	1.9	< 0.03	0.24

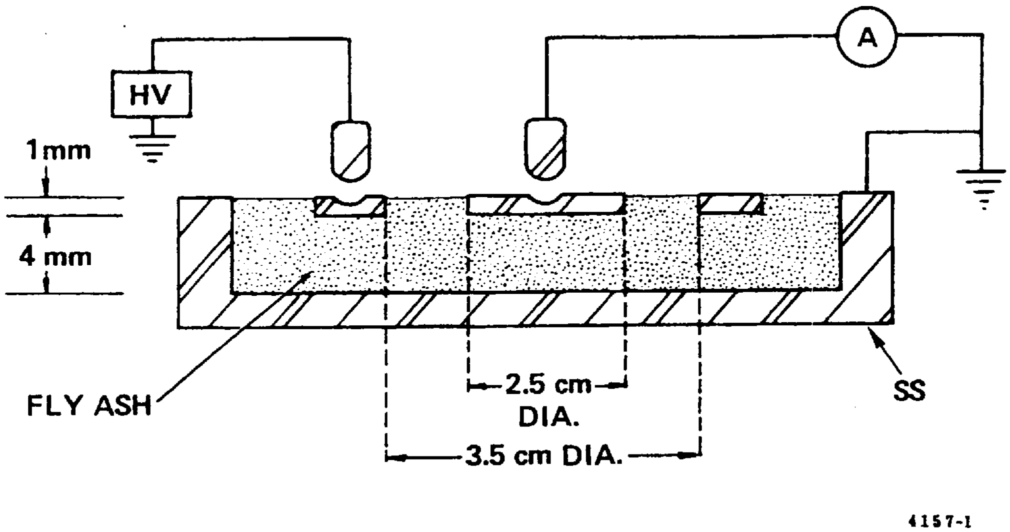

Figure 3-1. Radial cell for flyash SO_3 Conditioning Studies (8).

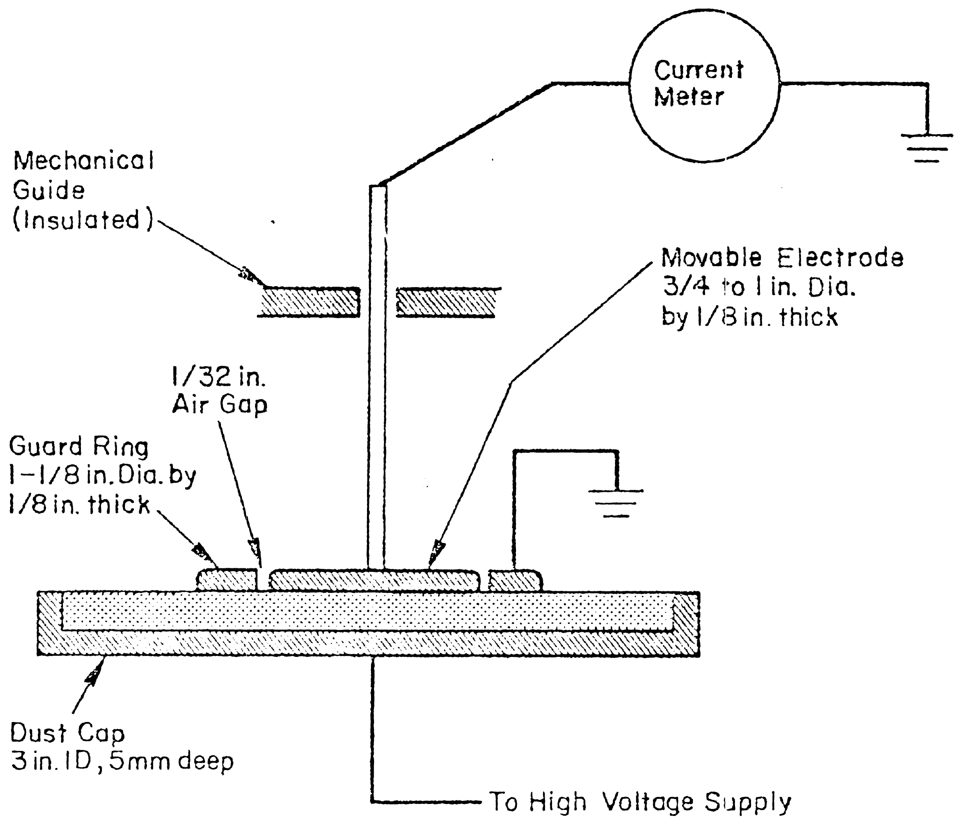

Figure-3-2. Standard Resistivity Cell (9).

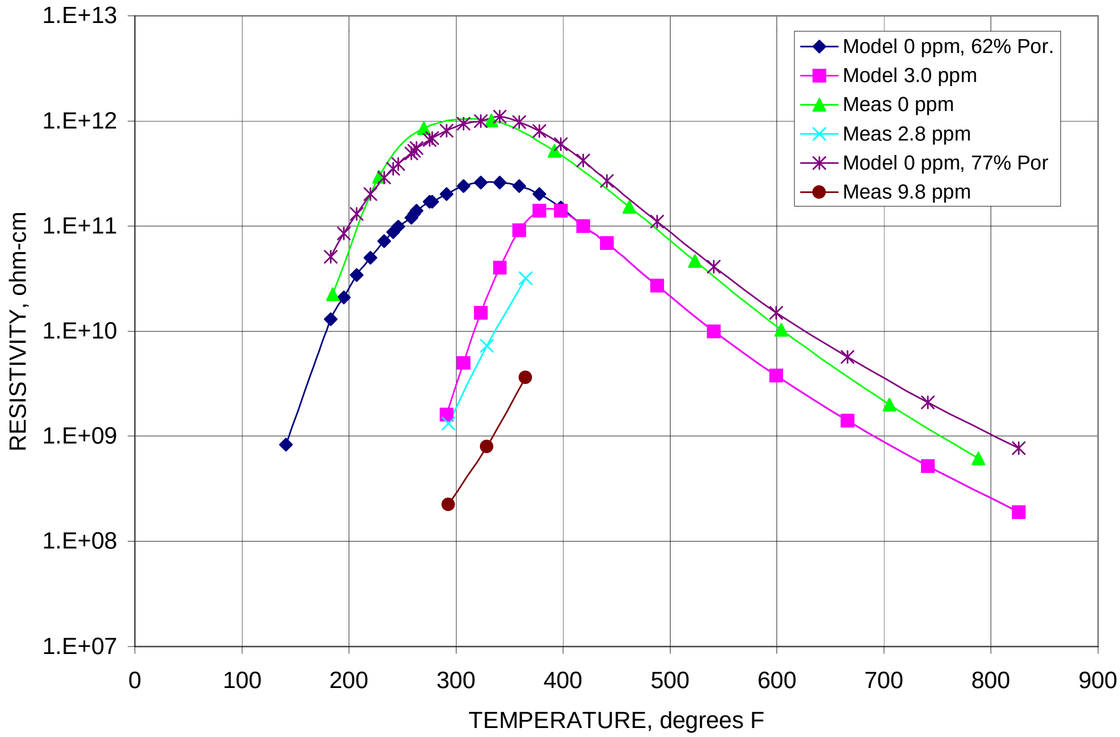

Figure-3-3. Comparison of measured results with and without SO_3 for Ash 9896-1-61 of the new set with the values predicted for that ash using the current (Version 2) resistivity model. Adjusting the porosity used in the model from the default value of 62% to 77% resulted in bringing the predicted values into accordance with the values measured (with the "radial" cell).

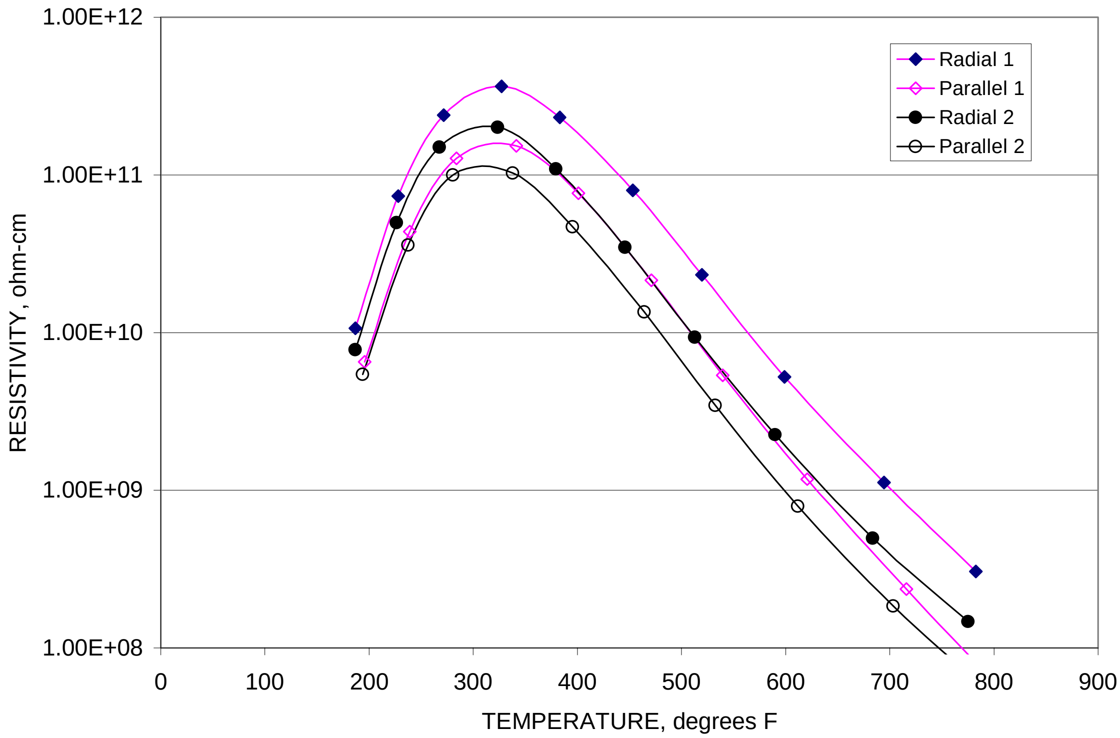

Figure 3-4. Descending resistivity curves for two ashes measured simultaneously with standard (parallel) and radial resistivity cells.

4
CONCLUSIONS AND RECOMMENDATIONS

A significant amount of new data has been generated with regard to the effect of SO_3 on flyash resistivity under laboratory conditions. These data will be used in the next phase of this project, in combination with the data previously published by Dr. Bickelhaupt, to generate new sets of correlations for use in predicting flyash resistivity in the presence of SO_3. It is expected that the new correlations, possibly including the new parameters of particle size and specific surface area, will allow the discontinuities in Dr. Bickelhaupt's original correlations to be avoided. It is suggested that predictions obtained with the new correlations be tested by comparison of predicted and measured results for a number of ashes. For example, Southern Research has several sets of measured data on hand for various client ashes for which laboratory resistivities have been measured, both with and without SO_3, but at too few conditions to make them useful in generating the new correlations. However, they would make good test cases for checking predictions from both the old and new predictive schemes.

In the course of this effort a discrepancy appears to have been found between laboratory measurements of resistivity with the standard parallel plate resistivity cell and the radial cell used in SO_3 studies. Descending temperature resistivity curves measured over the same range of conditions with the two cells in the absence of SO_3 seem to show systematically higher resistivity values at the same temperature when measured with the radial cell than with the standard cell. Further investigation of this discrepancy is suggested. Such investigation might include comparison of resistivities measured for the same ashes in the field and laboratory to see which, if either, of the two cells provides data that best correlates with field resistivities. If the radial cell data appear to better match field resistivities, it may be desirable to develop new "radial cell" correlations for predicting resistivity *versus* temperature in the absence of SO_3 in addition to the current effort in the presence of SO_3.

5
REFERENCES

1) Cushing, K. M. and J. D. McCain. "Fly Ash Property Study: Preliminary Findings." EPRI Technical Engineering Report No. TE-114557. Interim Report, December 1999. Electric Power Research Institute, Palo Alto, CA.

2) Bickelhaupt, R. E. "Electrical Volume Conduction in Fly Ash." Journal of the Air Pollution Control Association, Volume 24, Number 3, March 1974, pp. 251 – 255.

3) Bickelhaupt, R. E. "Surface Resistivity and the Chemical Composition of Fly Ash." Journal of the Air Pollution Control Association, Volume 25, Number 2, February 1975, pp.148 – 152.

4) Bickelhaupt, R. E. "A Technique for Predicting Fly Ash Resistivity." U. S. EPA Report Number EPA-600/7-79-204, August 1979, 114 pp.

5) Bickelhaupt, R. E. "Fly Ash Resistivity Prediction Improvement with Emphasis on the Effect of Sulfur Trioxide." U. S. Environmental Protection Agency Report Number EPA-600/7-86-010, NTIS PB 86-178126, March 1986.

6) Bickelhaupt, R. E. "Observations of Modeled and Laboratory Measured Resistivity." In Proceedings: The Eighth Symposium on the Transfer and Utilization of Particulate Control Technology, March 20-23, 1990, San Diego, CA. Electric Power Research Institute, Palo Alto, CA.

7) Bickelhaupt, R. E. "A Method for Predicting the Effective Volume Resistivity of Sodium-Depleted Fly Ash Layers in Hot-Side Electrostatic Precipitators." Electric Power Research Institute Report Number CS-3421, March 1984.

8) Bickelhaupt, R. E. "Measurement of Fly Ash Resistivity Using Simulated Flue Gas Environments." U. S. EPA Report Number EPA-600/7-78-035, March 1978, 29 pp.

9) Nichols, G. B. "Techniques for Measuring Fly Ash Resistivity." U. S. EPA Report Number EPA-650/2-74-079, August 1974, 49 pp.

Appendix A

Tables of measured sample resistivities *versus* temperature and SO_3 concentration

Table A-1. Sample 9896-1-57 Resistivity Data Summary

Descending temperature mode at 10.0 volume % H_2O, 0 ppm SO_3	
Temperature, °F	Resistivity,ohm cm
835	1.47×10^{9}
714	6.95×10^{9}
610	2.73×10^{10}
514	6.82×10^{10}
442	1.06×10^{11}
376	1.01×10^{11}
320	5.88×10^{10}
261	2.25×10^{10}
217	4.78×10^{9}
187	4.66×10^{8}

After equilibration at 10.0 volume % H_2O, 2.8 ppm SO_3	
Temperature, °F	Resistivity,ohm cm
365	2.46×10^{9}
329	6.82×10^{8}
293	2.25×10^{8}

After equilibration at 10.0 volume % H_2O, 9.8 ppm SO_3	
Temperature, °F	Resistivity,ohm cm
365	$2.77 \text{ X } 10^{8}$
347	$1.32 \text{ X } 10^{8}$
329	$6.21 \text{ X } 10^{7}$
311	$2.94 \text{ X } 10^{7}$
293	$1.53 \text{ X } 10^{7}$

Table A-2. Sample 9896-1-58 Resistivity Data Summary

Descending temperature mode at 10.0 volume % H_2O, 0 ppm SO_3	
Temperature, °F	Resistivity,ohm cm
829	3.18×10^{9}
718	1.66×10^{10}
619	5.70×10^{10}
527	1.39×10^{11}
455	2.06×10^{11}
388	2.12×10^{11}
331	1.36×10^{11}
271	4.11×10^{10}
228	7.96×10^{9}
187	1.01×10^{9}

After equilibration at 10.0 volume % H_2O, 2.8 ppm SO_3	
Temperature, °F	Resistivity,ohm cm
365	1.66×10^{9}
329	5.38×10^{8}
293	1.59×10^{8}

After equilibration at 10.0 volume % H_2O, 9.8 ppm SO_3	
Temperature, °F	Resistivity,ohm cm
365	5.23×10^{8}
347	1.91×10^{8}
329	9.32×10^{7}
311	4.49×10^{7}
293	2.25×10^{7}

Table A-3. Sample 9896-1-59 Resistivity Data Summary

Descending temperature mode at 10.0 volume % H_2O, 0 ppm SO_3	
Temperature, °F	Resistivity,ohm cm
824	4.90×10^{9}
714	2.55×10^{10}
613	9.32×10^{10}
523	2.39×10^{11}
451	3.82×10^{11}
387	4.39×10^{11}
329	3.47×10^{11}
270	1.41×10^{11}
226	3.32×10^{10}
187	3.47×10^{9}

After equilibration at 10.0 volume % H_2O, 2.8 ppm SO_3	
Temperature, °F	Resistivity,ohm cm
365	4.34×10^{9}
329	1.96×10^{9}
293	5.23×10^{8}

After equilibration at 10.0 volume % H_2O, 9.8 ppm SO_3	
Temperature, °F	Resistivity,ohm cm
365	1.19×10^{9}
347	5.79×10^{8}
329	2.83×10^{8}
311	1.34×10^{8}
293	6.47×10^{7}

Table A-4. Sample 9896-1-60 Resistivity Data Summary

Descending temperature mode at 10.0 volume % H_2O, 0 ppm SO_3	
Temperature, °F	Resistivity,ohm cm
817	2.94×10^{9}
707	1.78×10^{10}
608	7.96×10^{10}
520	2.55×10^{11}
448	5.54×10^{11}
383	8.68×10^{11}
327	9.32×10^{11}
268	5.79×10^{11}
226	1.74×10^{11}
185	1.78×10^{10}

After equilibration at 10.0 volume % H_2O, 2.8 ppm SO_3	
Temperature, °F	Resistivity,ohm cm
365	5.62×10^{9}
329	2.12×10^{9}
293	5.16×10^{8}

After equilibration at 10.0 volume % H_2O, 9.8 ppm SO_3	
Temperature, °F	Resistivity,ohm cm
365	1.01×10^{9}
347	4.78×10^{8}
329	2.25×10^{8}
311	1.11×10^{8}
293	5.92×10^{7}

Table A-5. Sample 9896-1-61 Resistivity Data Summary

Descending temperature mode at 10.1 volume % H_2O, 0 ppm SO_3	
Temperature, °F	Resistivity,ohm cm
788	6.16×10^{8}
705	2.01×10^{9}
604	1.03×10^{10}
523	4.66×10^{10}
462	1.53×10^{11}
392	5.16×10^{11}
333	1.01×10^{12}
270	8.49×10^{11}
228	2.94×10^{11}
185	2.25×10^{10}

After equilibration at 10.1 volume % H_2O, 2.9 ppm SO_3	
Temperature, °F	Resistivity,ohm cm
365	3.18×10^{10}
329	7.21×10^{9}
293	1.32×10^{9}

After equilibration at 10.1 volume % H_2O, 11.2 ppm SO_3	
Temperature, °F	Resistivity,ohm cm
365	3.64×10^{9}
329	7.96×10^{8}
293	2.25×10^{8}

Table A-6. Sample 9896-1-67 Resistivity Data Summary

Descending temperature mode at 10.1 volume % H_2O, 0 ppm SO_3	
Temperature, °F	Resistivity,ohm cm
783	1.74×10^{9}
700	6.37×10^{9}
601	3.47×10^{10}
520	1.41×10^{11}
459	3.94×10^{11}
388	1.06×10^{12}
331	1.66×10^{12}
268	1.19×10^{12}
216	3.82×10^{11}
176	3.18×10^{10}

After equilibration at 10.1 volume % H_2O, 2.9 ppm SO_3	
Temperature, °F	Resistivity,ohm cm
365	3.64×10^{10}
329	1.00×10^{10}
293	1.78×10^{9}

After equilibration at 10.1 volume % H_2O, 11.2 ppm SO_3	
Temperature, °F	Resistivity,ohm cm
365	5.42×10^{9}
329	1.14×10^{9}
293	2.18×10^{8}

Table A-7. Sample 9896-1-68 Resistivity Data Summary

Descending temperature mode at 10.2 volume % H_2O, 0 ppm SO_3	
Temperature, °F	Resistivity,ohm cm
795	1.63×10^{9}
698	7.49×10^{9}
603	3.82×10^{10}
522	1.32×10^{11}
459	3.06×10^{11}
390	4.90×10^{11}
331	4.34×10^{11}
273	1.82×10^{11}
228	4.39×10^{10}
189	5.46×10^{9}

After equilibration at 10.2 volume % H_2O, 2.6 ppm SO_3	
Temperature, °F	Resistivity,ohm cm
365	3.47×10^{9}
329	8.88×10^{8}
293	2.32×10^{8}

After equilibration at 10.2 volume % H_2O, 10.7 ppm SO_3	
Temperature, °F	Resistivity,ohm cm
365	2.18×10^{8}
329	7.21×10^{7}
293	2.46×10^{7}

Table A-8. Sample 9896-1-69 Resistivity Data Summary

Descending temperature mode at 10.1 volume % H_2O, 0 ppm SO_3	
Temperature, °F	Resistivity,ohm cm
777	6.95×10^{8}
694	2.12×10^{9}
595	8.30×10^{9}
516	2.32×10^{10}
455	3.82×10^{10}
385	4.15×10^{10}
329	2.55×10^{10}
268	5.54×10^{9}
226	1.23×10^{9}
183	2.12×10^{8}

After equilibration at 10.1 volume % H_2O, 2.9 ppm SO_3	
Temperature, °F	Resistivity,ohm cm
365	2.83×10^{9}
329	1.23×10^{9}
293	6.76×10^{8}

After equilibration at 10.1 volume % H_2O, 11.2 ppm SO_3	
Temperature, °F	Resistivity,ohm cm
365	4.72×10^{8}
329	1.63×10^{8}
293	4.20×10^{7}

Table A-9. Sample 9896-1-70 Resistivity Data Summary

Descending temperature mode at 10.1 volume % H_2O, 0 ppm SO_3	
Temperature, °F	Resistivity,ohm cm
772	1.91×10^{9}
689	5.79×10^{9}
592	2.39×10^{10}
513	7.35×10^{10}
453	1.47×10^{11}
381	2.18×10^{11}
327	1.82×10^{11}
266	6.59×10^{10}
225	1.82×10^{10}
183	2.12×10^{9}

After equilibration at 10.1 volume % H_2O, 2.9 ppm SO_3	
Temperature, °F	Resistivity,ohm cm
365	1.25×10^{9}
329	3.94×10^{8}
293	1.91×10^{8}

After equilibration at 10.1 volume % H_2O, 11.2 ppm SO_3	
Temperature, °F	Resistivity,ohm cm
365	2.73×10^{8}
329	9.79×10^{7}
293	4.34×10^{7}

Table A-10. Sample 9896-1-121 Resistivity Data Summary

Descending temperature mode at 10.0 volume % H_2O, 0 ppm SO_3	
Temperature, °F	Resistivity,ohm cm
788	1.41×10^{9}
685	6.59×10^{9}
601	2.94×10^{10}
518	1.36×10^{11}
457	4.66×10^{11}
388	1.66×10^{12}
333	3.18×10^{12}
270	3.18×10^{12}
228	1.09×10^{12}
187	1.14×10^{11}

After equilibration at 10.0 volume % H_2O, 2.7 ppm SO_3	
Temperature, °F	Resistivity,ohm cm
365	1.53×10^{12}
329	5.62×10^{11}
293	4.42×10^{10}

After equilibration at 10.0 volume % H_2O, 10.0 ppm SO_3	
Temperature, °F	Resistivity,ohm cm
365	7.35×10^{11}
329	9.79×10^{10}
293	3.84×10^{8}

Table A-11. Sample 9896-1-122 Resistivity Data Summary

Descending temperature mode at 10.0 volume % H_2O, 0 ppm SO_3	
Temperature, °F	Resistivity,ohm cm
781	1.16×10^{9}
680	5.20×10^{9}
595	2.12×10^{10}
514	8.30×10^{10}
453	2.39×10^{11}
385	5.88×10^{11}
331	8.88×10^{11}
268	6.47×10^{11}
226	2.39×10^{11}
187	3.90×10^{10}

After equilibration at 10.0 volume % H_2O, 2.7 ppm SO_3	
Temperature, °F	Resistivity,ohm cm
365	9.32×10^{9}
329	3.47×10^{9}
293	7.96×10^{8}

After equilibration at 10.0 volume % H_2O, 10.0 ppm SO_3	
Temperature, °F	Resistivity,ohm cm
365	3.11×10^{9}
329	5.46×10^{8}
293	8.30×10^{7}

Table A-12. Sample 9896-1-123 Resistivity Data Summary

Descending temperature mode at 10.2 volume % H_2O, 0 ppm SO_3	
Temperature, °F	Resistivity,ohm cm
790	1.59×10^{9}
693	6.16×10^{9}
597	2.94×10^{10}
518	1.01×10^{11}
455	2.25×10^{11}
388	3.32×10^{11}
329	2.63×10^{11}
271	9.79×10^{10}
228	2.06×10^{10}
189	2.25×10^{9}

After equilibration at 10.2 volume % H_2O, 2.6 ppm SO_3	
Temperature, °F	Resistivity,ohm cm
365	8.99×10^{8}
329	3.18×10^{8}
293	8.13×10^{7}

After equilibration at 10.2 volume % H_2O, 10.7 ppm SO_3	
Temperature, °F	Resistivity,ohm cm
365	1.66×10^{8}
329	4.44×10^{7}
293	1.12×10^{7}

Table A-13. Sample 9896-1-124 Resistivity Data Summary

Descending temperature mode at 10.2 volume % H_2O, 0 ppm SO_3	
Temperature, °F	Resistivity,ohm cm
784	2.25×10^{8}
685	1.05×10^{9}
594	5.27×10^{9}
514	2.25×10^{10}
451	6.37×10^{10}
385	1.41×10^{11}
327	1.53×10^{11}
271	7.07×10^{10}
226	1.56×10^{10}
187	1.66×10^{9}

After equilibration at 10.2 volume % H_2O, 2.6 ppm SO_3	
Temperature, °F	Resistivity,ohm cm
365	1.50×10^{9}
329	5.88×10^{8}
293	2.25×10^{8}

After equilibration at 10.2 volume % H_2O, 10.7 ppm SO_3	
Temperature, °F	Resistivity,ohm cm
365	2.12×10^{8}
329	8.78×10^{7}
293	4.78×10^{7}

Table A-14. Sample 9896-1-130 Resistivity Data Summary

Descending temperature mode at 10.0 volume % H_2O, 0 ppm SO_3	
Temperature, °F	Resistivity,ohm cm
775	3.94×10^{9}
675	1.70×10^{10}
590	5.16×10^{10}
511	1.21×10^{11}
450	1.74×10^{11}
383	1.56×10^{11}
329	8.22×10^{10}
268	1.82×10^{10}
226	3.64×10^{9}
187	4.55×10^{8}

After equilibration at 10.0 volume % H_2O, 2.7 ppm SO_3	
Temperature, °F	Resistivity,ohm cm
365	5.31×10^{8}
329	2.01×10^{8}
293	9.32×10^{7}

After equilibration at 10.0 volume % H_2O, 10.0 ppm SO_3	
Temperature, °F	Resistivity,ohm cm
365	1.47×10^{8}
329	4.87×10^{7}
293	1.70×10^{7}

Table A-15. Sample 9896-1-133 Resistivity Data Summary

Descending temperature mode at 10.0 volume % H_2O, 0 ppm SO_3	
Temperature, °F	Resistivity,ohm cm
770	5.46×10^{8}
669	2.55×10^{9}
586	1.08×10^{10}
507	4.60×10^{10}
448	1.29×10^{11}
381	3.06×10^{11}
327	3.82×10^{11}
266	2.12×10^{11}
225	6.06×10^{10}
185	6.37×10^{9}

After equilibration at 10.0 volume % H_2O, 2.7 ppm SO_3	
Temperature, °F	Resistivity,ohm cm
365	4.34×10^{10}
329	1.47×10^{10}
293	2.55×10^{9}

After equilibration at 10.0 volume % H_2O, 10.0 ppm SO_3	
Temperature, °F	Resistivity,ohm cm
365	7.64×10^{9}
329	2.12×10^{9}
293	4.75×10^{7}

Table A-16. Sample D492A Resistivity Data Summary

Descending temperature mode at 10.4 volume % H_2O, 0 ppm SO_3	
Temperature, °F	Resistivity,ohm cm
784	4.24×10^{8}
698	1.53×10^{9}
601	8.13×10^{9}
527	3.64×10^{10}
457	1.56×10^{11}
387	5.97×10^{11}
331	1.27×10^{12}
268	9.67×10^{11}
228	2.63×10^{11}
187	1.39×10^{10}

After equilibration at 10.4 volume % H_2O, 3.0 ppm SO_3	
Temperature, °F	Resistivity,ohm cm
300	9.79×10^{11}
270	2.83×10^{8}

Table A-17. Sample 301 Resistivity Data Summary

Descending temperature mode at 9.9 volume % H_2O, 0 ppm SO_3	
Temperature, °F	Resistivity,ohm cm
185	4.85×10^{10}
235	3.06×10^{11}
290	6.50×10^{11}
359	5.12×10^{11}
440	2.11×10^{11}
563	3.36×10^{10}
665	6.98×10^{9}
826	8.25×10^{8}

After equilibration at 9.9 volume % H_2O, 1.5 ppm SO_3	
Temperature, °F	Resistivity,ohm cm
257	7.55×10^{10}
269	2.51×10^{11}

After equilibration at 9.4 volume % H_2O, 4.2 ppm SO_3	
Temperature, °F	Resistivity,ohm cm
266	5.63×10^{10}
277	7.50×10^{10}
278	1.50×10^{11}
290	2.70×10^{11}
287	2.95×10^{11}

After equilibration at 9.8 volume % H_2O, 9.6 ppm SO_3	
Temperature, °F	Resistivity,ohm cm
281	4.17×10^{9}
284	8.09×10^{9}
284	1.06×10^{10}
297	3.89×10^{10}
323	2.51×10^{11}
323	3.54×10^{11}
326	6.09×10^{11}

Table A-18. Sample 302 Resistivity Data Summary

Descending temperature mode at 9.9 volume % H_2O, 0 ppm SO_3	
Temperature, °F	Resistivity,ohm cm
185	2.10×10^{11}
238	1.59×10^{12}
293	2.73×10^{12}
362	2.67×10^{12}
445	1.38×10^{12}
546	3.51×10^{11}
679	5.09×10^{10}
835	7.03×10^{9}

After equilibration at 9.9 volume % H_2O, 1.2 ppm SO_3	
Temperature, °F	Resistivity,ohm cm
243	4.89×10^{8}
272	4.20×10^{9}
300	6.34×10^{10}

After equilibration at 9.4 volume % H_2O, 3.4 ppm SO_3	
Temperature, °F	Resistivity,ohm cm
266	1.44×10^{8}
287	3.13×10^{9}
300	2.01×10^{10}

After equilibration at 9.8 volume % H_2O, 8.9 ppm SO_3	
Temperature, °F	Resistivity,ohm cm
287	1.75×10^{8}
330	1.73×10^{10}
351	1.11×10^{11}

Table A-19. Sample 303 Resistivity Data Summary

Descending temperature mode at 9.9 volume % H_2O, 0 ppm SO_3	
Temperature, °F	Resistivity,ohm cm
193	3.27×10^{10}
244	2.17×10^{11}
302	7.46×10^{11}
371	1.37×10^{12}
455	1.13×10^{12}
590	4.18×10^{11}
685	1.62×10^{11}
758	4.94×10^{10}
851	1.58×10^{10}

After equilibration at 9.9 volume % H_2O, 1.5 ppm SO_3	
Temperature, °F	Resistivity,ohm cm
260	9.06×10^{8}
297	5.45×10^{9}
338	8.04×10^{10}

After equilibration at 9.4 volume % H_2O, 4.2 ppm SO_3	
Temperature, °F	Resistivity,ohm cm
279	4.49×10^{8}
314	2.97×10^{9}
353	3.12×10^{10}

After equilibration at 9.8 volume % H_2O, 9.6 ppm SO_3	
Temperature, °F	Resistivity,ohm cm
287	6.62×10^{7}
321	9.51×10^{8}
361	8.04×10^{9}
402	4.94×10^{10}

Table A-20. Sample 304 Resistivity Data Summary

Descending temperature mode at 9.9 volume % H_2O, 0 ppm SO_3	
Temperature, °F	Resistivity,ohm cm
183	1.14×10^{11}
235	1.22×10^{12}
290	2.87×10^{12}
358	1.70×10^{12}
440	3.98×10^{11}
546	4.99×10^{10}
665	5.41×10^{9}
835	5.59×10^{8}

After equilibration at 9.9 volume % H_2O, 1.4 ppm SO_3	
Temperature, °F	Resistivity,ohm cm
243	2.03×10^{11}
255	2.62×10^{11}
266	2.00×10^{12}

After equilibration at 9.4 volume % H_2O, 4.0 ppm SO_3	
Temperature, °F	Resistivity,ohm cm
266	5.41×10^{9}
260	3.02×10^{10}
275	2.29×10^{11}
290	1.94×10^{12}

After equilibration at 9.8 volume % H_2O, 9.8 ppm SO_3	
Temperature, °F	Resistivity,ohm cm
281	4.32×10^{8}
287	1.69×10^{9}
284	7.71×10^{9}
300	1.77×10^{11}
320	1.20×10^{12}
320	1.40×10^{12}
323	2.42×10^{12}

Table A-21. Sample 305 Resistivity Data Summary

Descending temperature mode at 9.8 volume % H_2O, 0 ppm SO_3	
Temperature, °F	Resistivity,ohm cm
185	3.34×10^{10}
235	2.29×10^{11}
293	4.38×10^{11}
362	3.43×10^{11}
445	9.47×10^{10}
546	1.54×10^{10}
672	2.25×10^{9}
835	2.08×10^{8}

After equilibration at 9.8 volume % H_2O, 1.4 ppm SO_3	
Temperature, °F	Resistivity,ohm cm
260	1.53×10^{9}
300	2.67×10^{10}
333	1.79×10^{11}

After equilibration at 9.9 volume % H_2O, 3.9 ppm SO_3	
Temperature, °F	Resistivity,ohm cm
275	4.51×10^{8}
313	5.57×10^{9}
355	4.27×10^{10}

After equilibration at 9.9 volume % H_2O, 9.8 ppm SO_3	
Temperature, °F	Resistivity,ohm cm
286	1.65×10^{8}
326	2.14×10^{9}
362	1.36×10^{10}

Table A-22. Sample 306 Resistivity Data Summary

Descending temperature mode at 9.8 volume % H_2O, 0 ppm SO_3	
Temperature, °F	Resistivity,ohm cm
185	3.08×10^{10}
235	2.63×10^{11}
293	5.48×10^{11}
359	3.16×10^{11}
440	9.29×10^{10}
540	1.40×10^{10}
665	1.67×10^{9}
835	2.03×10^{8}

After equilibration at 9.8 volume % H_2O, 1.4 ppm SO_3	
Temperature, °F	Resistivity,ohm cm
257	2.86×10^{9}
293	4.79×10^{10}
330	2.29×10^{11}

After equilibration at 9.9 volume % H_2O, 3.9 ppm SO_3	
Temperature, °F	Resistivity,ohm cm
272	1.17×10^{9}
310	1.23×10^{10}
348	9.29×10^{10}

After equilibration at 9.9 volume % H_2O, 9.8 ppm SO_3	
Temperature, °F	Resistivity,ohm cm
284	4.56×10^{8}
320	5.03×10^{9}
359	3.00×10^{10}

Table A-23. Sample 307 Resistivity Data Summary

Descending temperature mode at 9.8 volume % H_2O, 0 ppm SO_3	
Temperature, °F	Resistivity,ohm cm
185	6.97×10^{8}
235	5.19×10^{9}
293	1.72×10^{10}
359	2.42×10^{10}
440	2.01×10^{10}
546	8.89×10^{9}
672	1.62×10^{9}
835	2.82×10^{8}

After equilibration at 9.8 volume % H_2O, 1.4 ppm SO_3	
Temperature, °F	Resistivity,ohm cm
257	3.07×10^{8}
293	8.90×10^{8}
330	2.34×10^{9}

After equilibration at 9.9 volume % H_2O, 3.9 ppm SO_3	
Temperature, °F	Resistivity,ohm cm
275	9.90×10^{7}
310	2.68×10^{8}
351	7.41×10^{8}

After equilibration at 9.9 volume % H_2O, 9.8 ppm SO_3	
Temperature, °F	Resistivity,ohm cm
284	2.70×10^{7}
320	1.11×10^{8}
359	2.23×10^{8}

Table A-24. Sample 308 Resistivity Data Summary

Descending temperature mode at 9.8 volume % H_2O, 0 ppm SO_3	
Temperature, °F	Resistivity,ohm cm
183	2.20×10^{8}
233	1.74×10^{9}
293	1.13×10^{10}
362	4.99×10^{10}
445	6.22×10^{10}
546	3.21×10^{10}
665	7.58×10^{9}
835	8.91×10^{8}

After equilibration at 9.8 volume % H_2O, 1.4 ppm SO_3	
Temperature, °F	Resistivity,ohm cm
257	1.70×10^{8}
293	8.90×10^{8}
330	2.74×10^{9}

After equilibration at 9.9 volume % H_2O, 3.9 ppm SO_3	
Temperature, °F	Resistivity,ohm cm
275	3.61×10^{7}
313	1.66×10^{8}
348	6.50×10^{8}

After equilibration at 9.9 volume % H_2O, 9.8 ppm SO_3	
Temperature, °F	Resistivity,ohm cm
284	1.55×10^{7}
320	6.19×10^{7}
362	2.05×10^{8}

Table A-25. Sample 311 Resistivity Data Summary

Descending temperature mode at 10.2 volume % H_2O, 0 ppm SO_3	
Temperature, °F	Resistivity,ohm cm
182	1.60×10^{10}
233	1.30×10^{11}
289	4.00×10^{11}
351	3.50×10^{11}
431	1.30×10^{11}
489	4.80×10^{10}
554	1.40×10^{10}
639	3.20×10^{9}
723	8.50×10^{8}
835	2.10×10^{8}

After equilibration at 9.6 volume % H_2O, 1.5 ppm SO_3	
Temperature, °F	Resistivity,ohm cm
258	4.30×10^{9}
294	6.00×10^{10}
331	2.80×10^{11}

After equilibration at 9.9 volume % H_2O, 4.0 ppm SO_3	
Temperature, °F	Resistivity,ohm cm
278	9.30×10^{8}
310	1.80×10^{10}
344	1.55×10^{11}

After equilibration at 9.7 volume % H_2O, 9.0 ppm SO_3	
Temperature, °F	Resistivity,ohm cm
286	4.00×10^{8}
324	6.30×10^{9}
359	4.80×10^{10}

Table A-26. Sample 312 Resistivity Data Summary

Descending temperature mode at 10.1 volume % H_2O, 0 ppm SO_3	
Temperature, °F	Resistivity,ohm cm
825	5.26×10^{9}
735	1.54×10^{10}
664	4.00×10^{10}
569	2.06×10^{11}
499	6.34×10^{11}
450	1.09×10^{12}
368	2.68×10^{12}
302	3.78×10^{12}
242	2.15×10^{12}
184	1.57×10^{11}

After equilibration at 9.6 volume % H_2O, 1.5 ppm SO_3	
Temperature, °F	Resistivity,ohm cm
258	2.34×10^{10}
298	1.78×10^{11}
334	8.71×10^{11}

After equilibration at 9.9 volume % H_2O, 4.0 ppm SO_3	
Temperature, °F	Resistivity,ohm cm
275	4.66×10^{9}
310	5.78×10^{10}
343	3.71×10^{11}

After equilibration at 9.7 volume % H_2O, 9.0 ppm SO_3	
Temperature, °F	Resistivity,ohm cm
284	1.24×10^{9}
323	3.37×10^{10}
363	2.22×10^{11}

Appendix B

Plots of Resistivity *versus* Temperature at Various SO_3 Concentrations

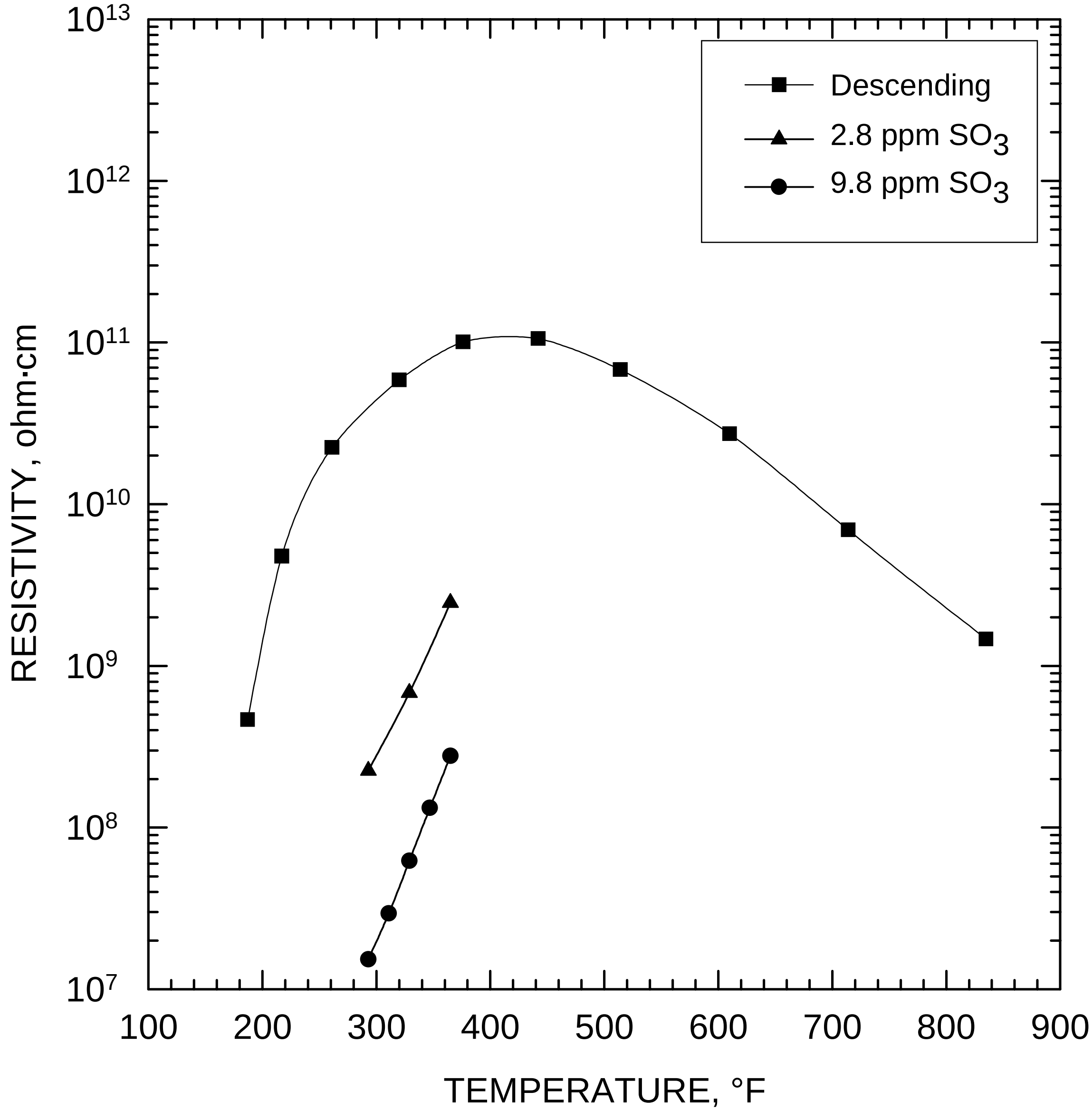

Figure B-1. Laboratory resistivity of Sample 9896-1-57 with 10.0 % water by volume and two SO_3 injection rates at specific temperatures.

.

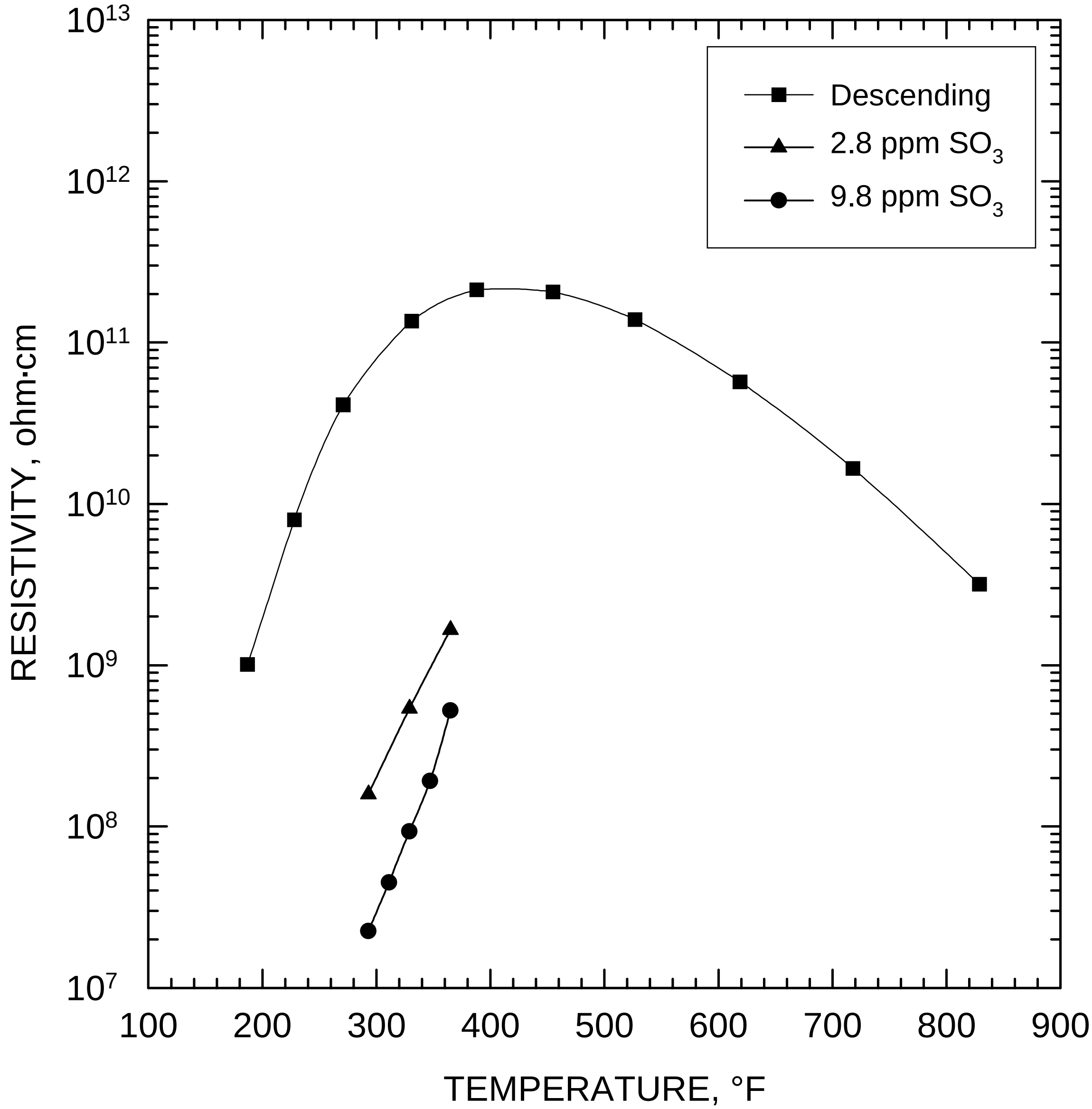

Figure B-2. Laboratory resistivity of Sample 9896-1-58 with 10.0 % water by volume and two SO_3 injection rates at specific temperatures.

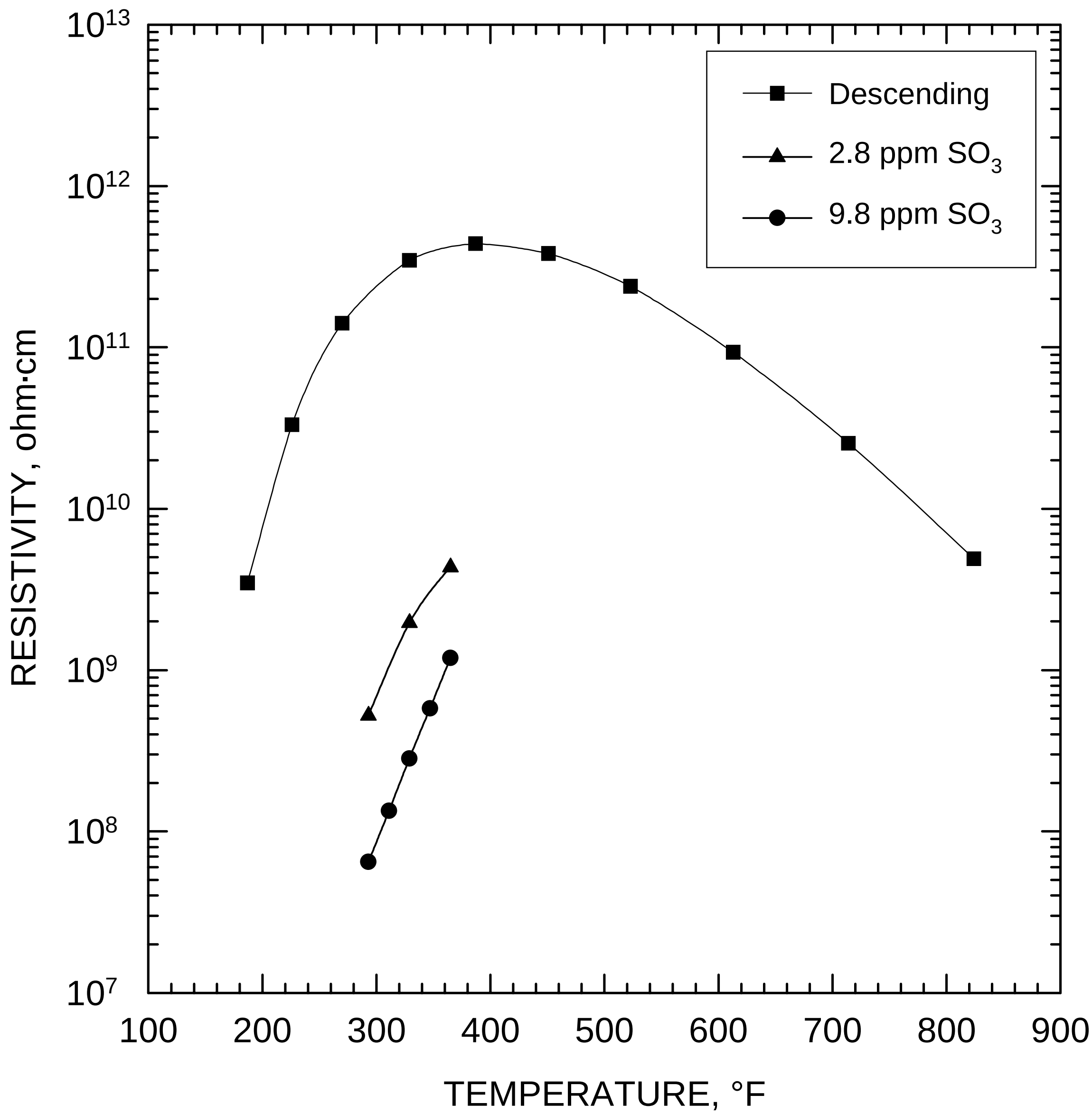

Figure B-3. Laboratory resistivity of Sample 9896-1-59 with 10.0 % water by volume and two SO_3 injection rates at specific temperatures.

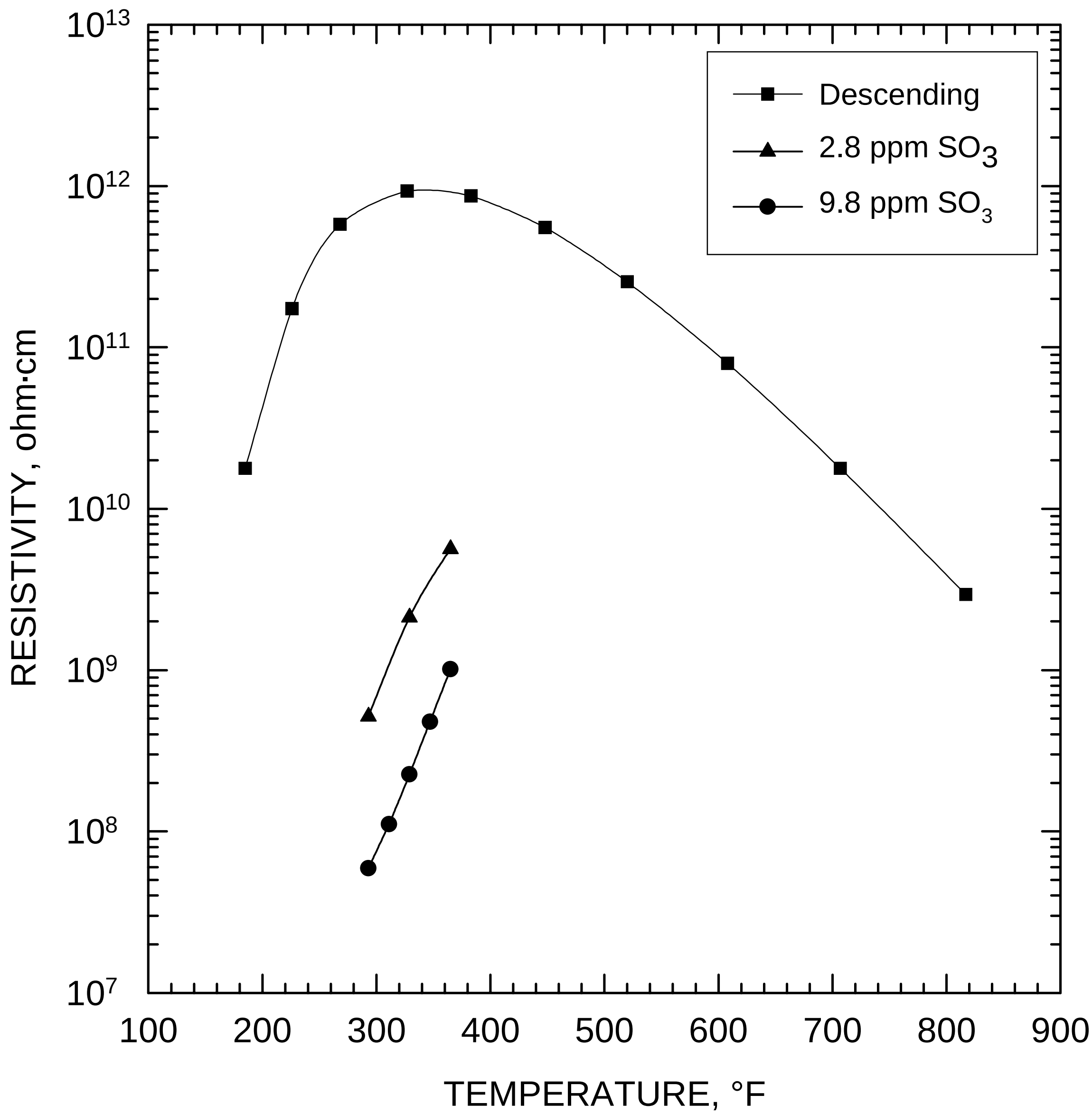

Figure B-4. Laboratory resistivity of Sample 9896-1-60 with 10.0 % water by volume and two SO_3 injection rates at specific temperatures.

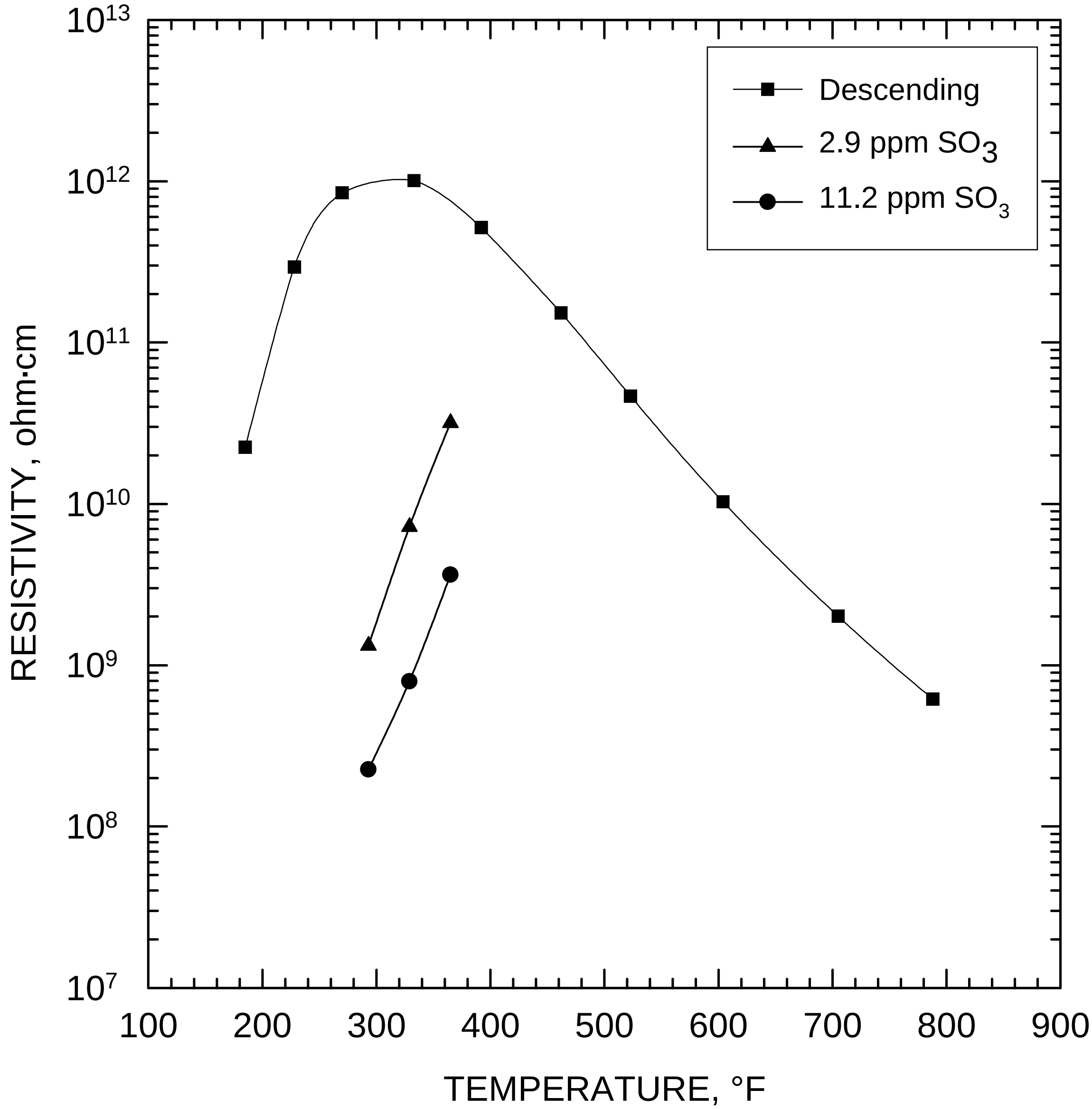

Figure B-5. Laboratory resistivity of Sample 9896-1-61 with 10.1 % water by volume and two SO_3 injection rates at specific temperatures.

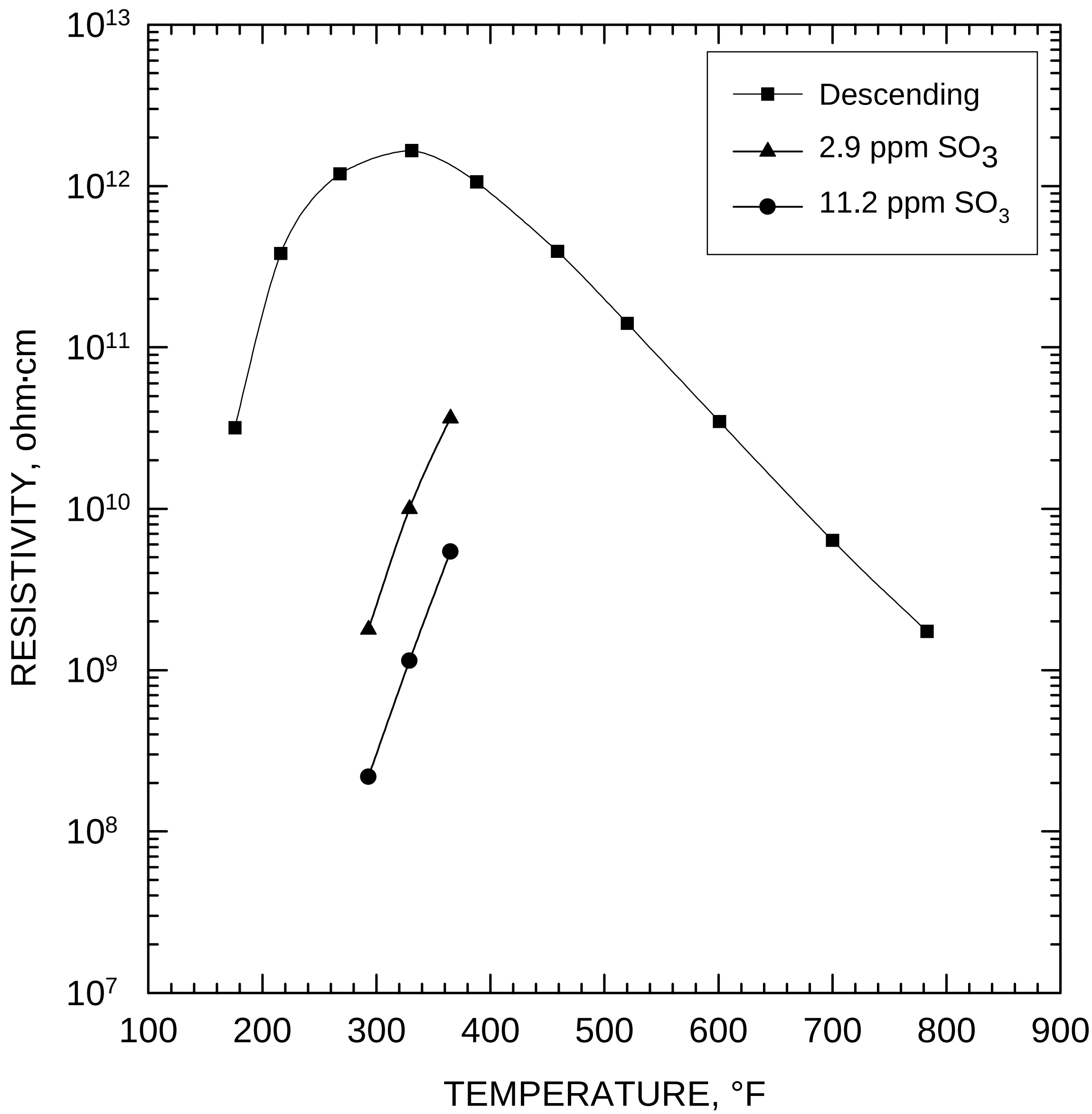

Figure B-6. Laboratory resistivity of Sample 9896-1-67 with 10.1 % water by volume and two SO_3 injection rates at specific temperatures.

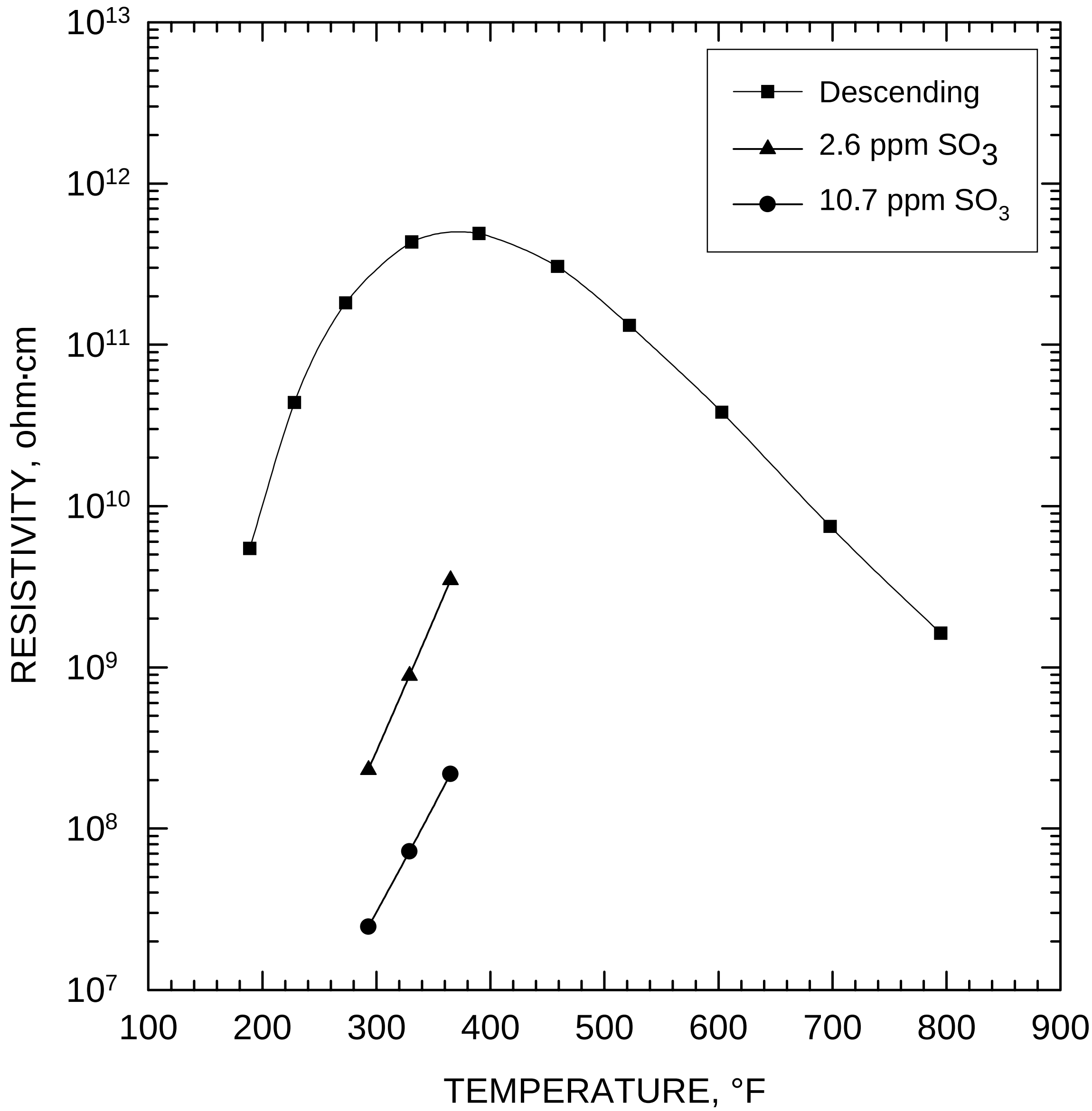

Figure B-7. Laboratory resistivity of Sample 9896-1-68 with 10.2 % water by volume and two SO_3 injection rates at specific temperatures.

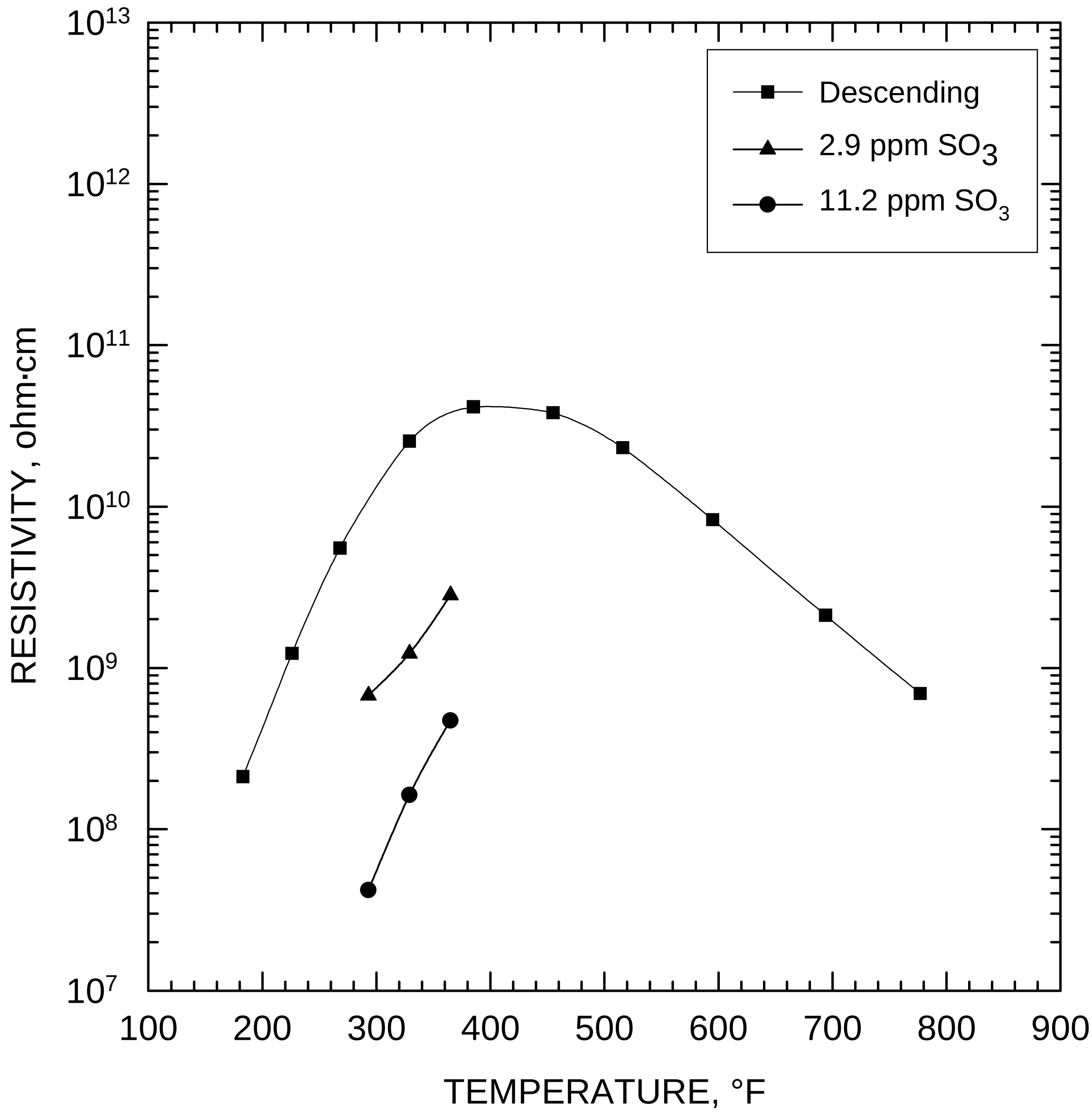

Figure B-8. Laboratory resistivity of Sample 9896-1-69 with 10.1 % water by volume and two SO_3 injection rates at specific temperatures.

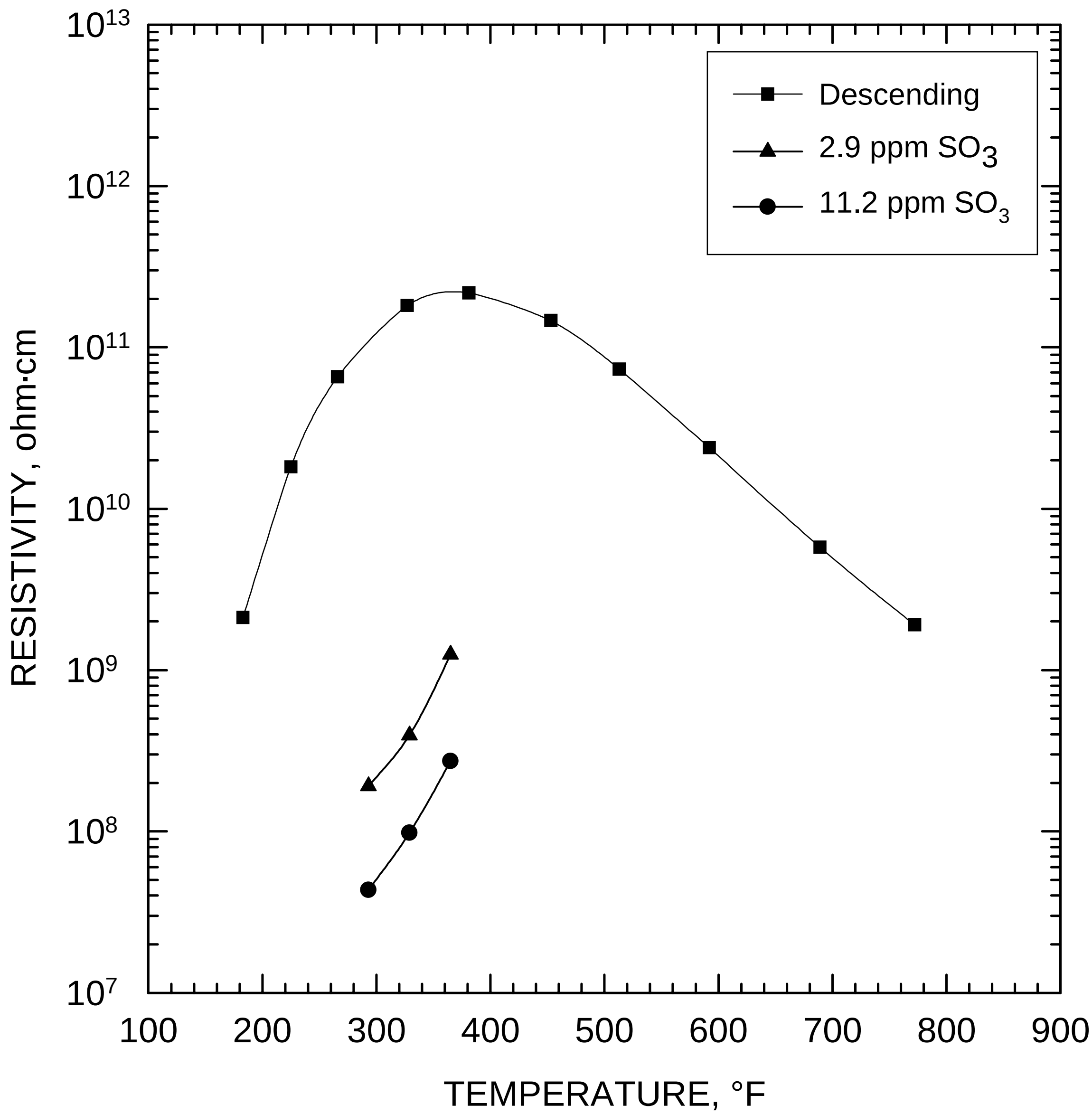

Figure B-9. Laboratory resistivity of Sample 9896-1-70 with 10.1 % water by volume and two SO_3 injection rates at specific temperatures.

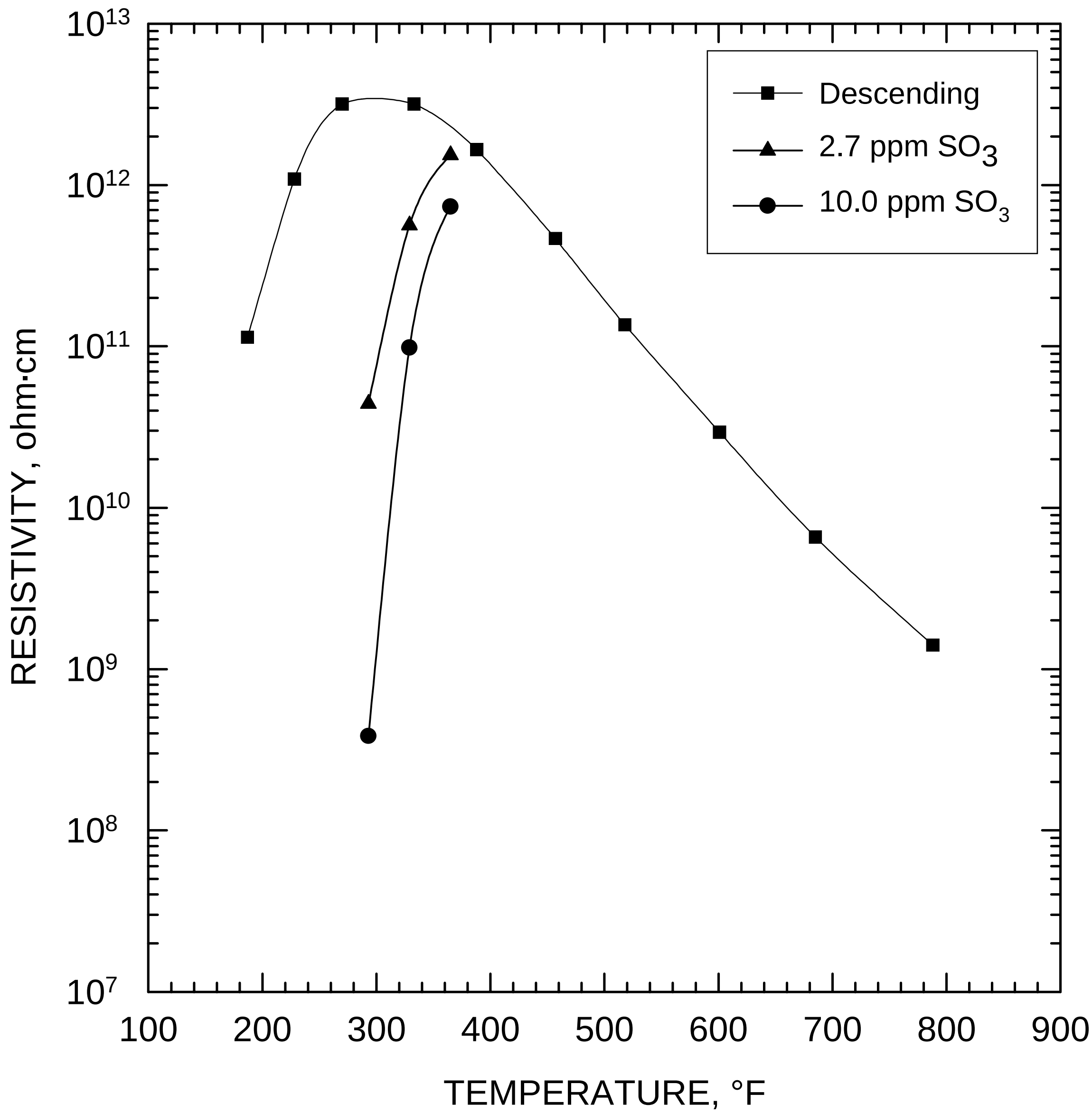

Figure B-10. Laboratory resistivity of Sample 9896-1-121 with 10.0 % water by volume and two SO_3 injection rates at specific temperatures.

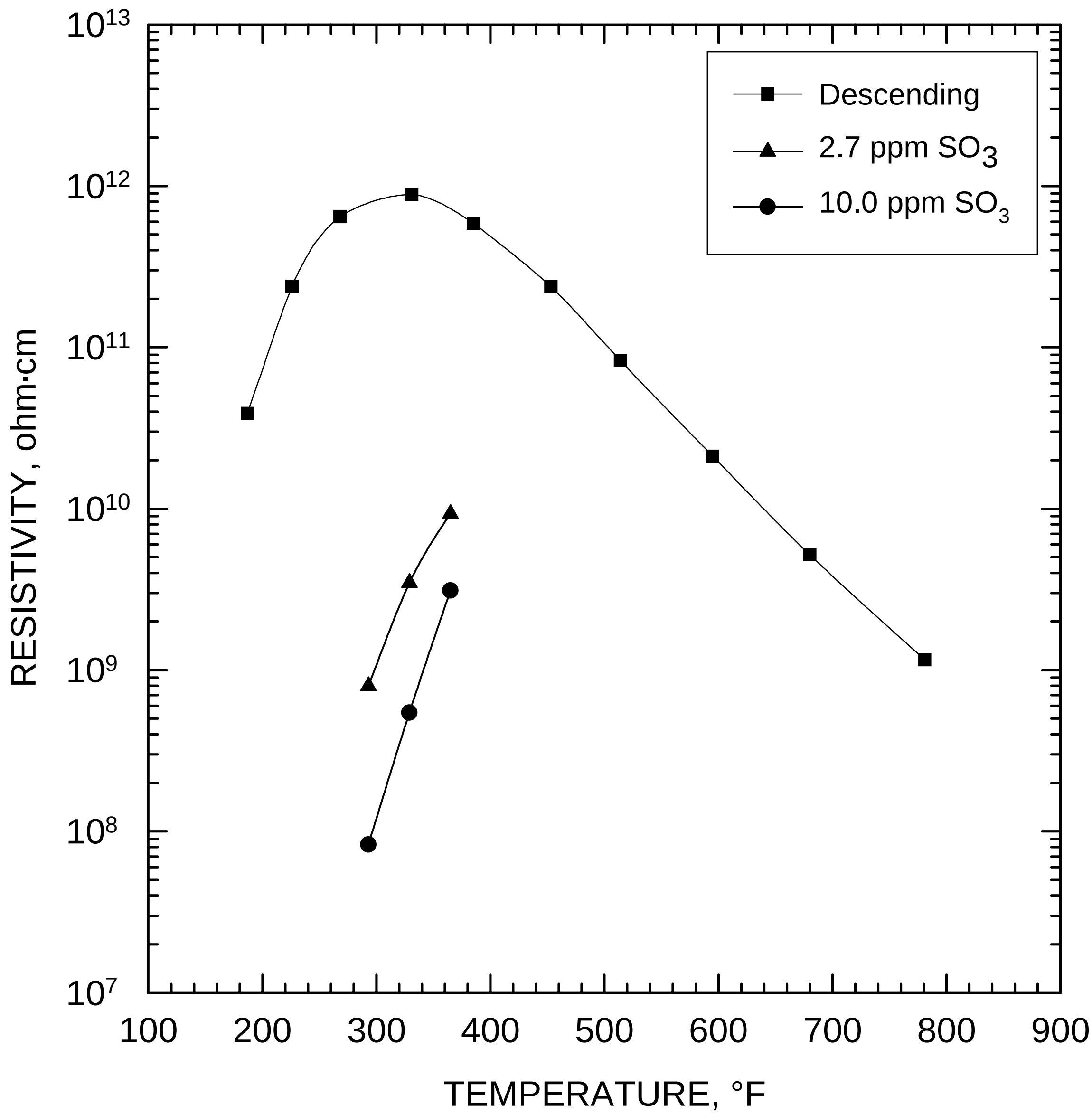

Figure B-11. Laboratory resistivity of Sample 9896-1-122 with 10.0 % water by volume and two SO_3 injection rates at specific temperatures.

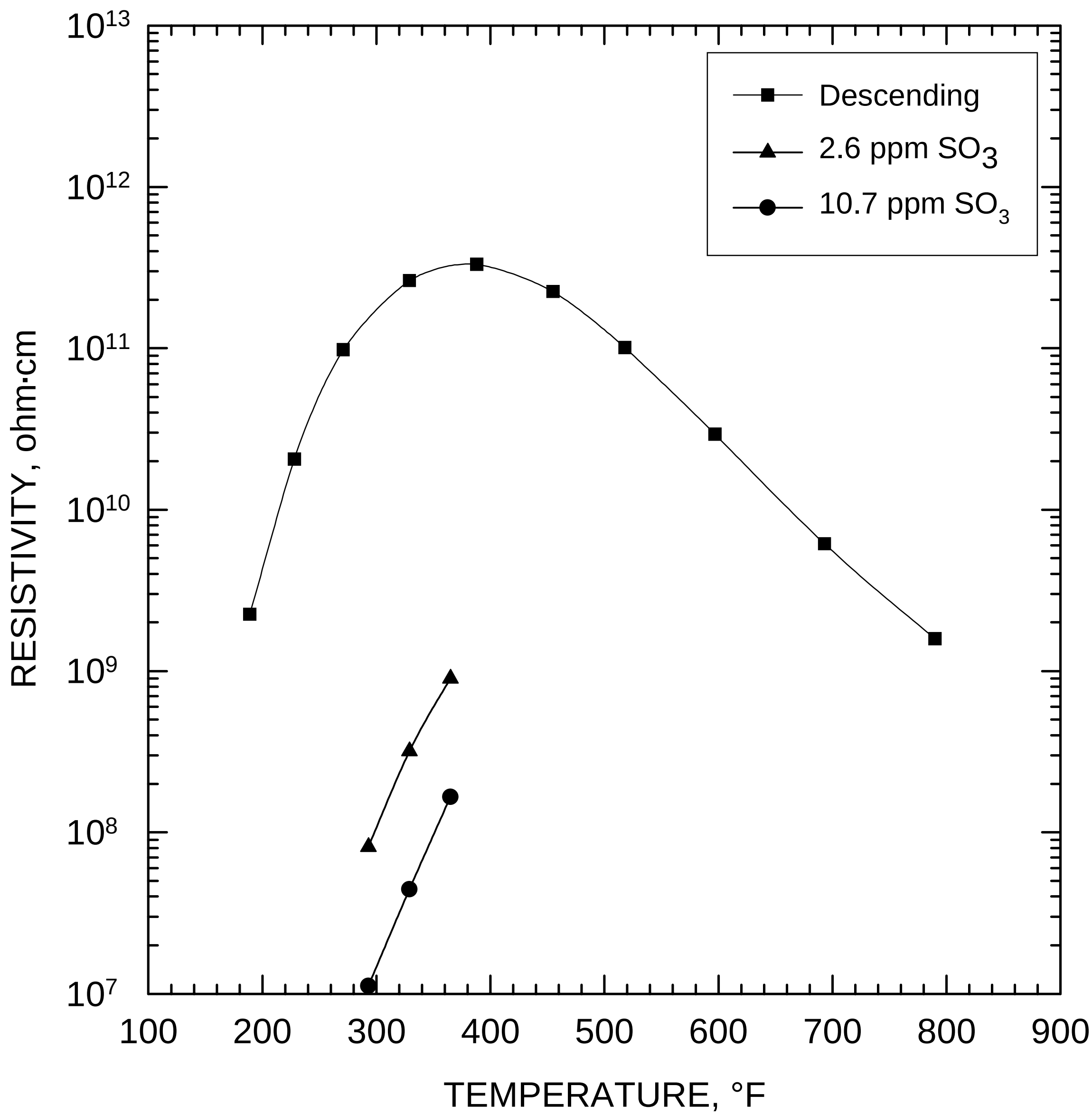

Figure B-12. Laboratory resistivity of Sample 9896-1-123 with 10.2 % water by volume and two SO_3 injection rates at specific temperatures.

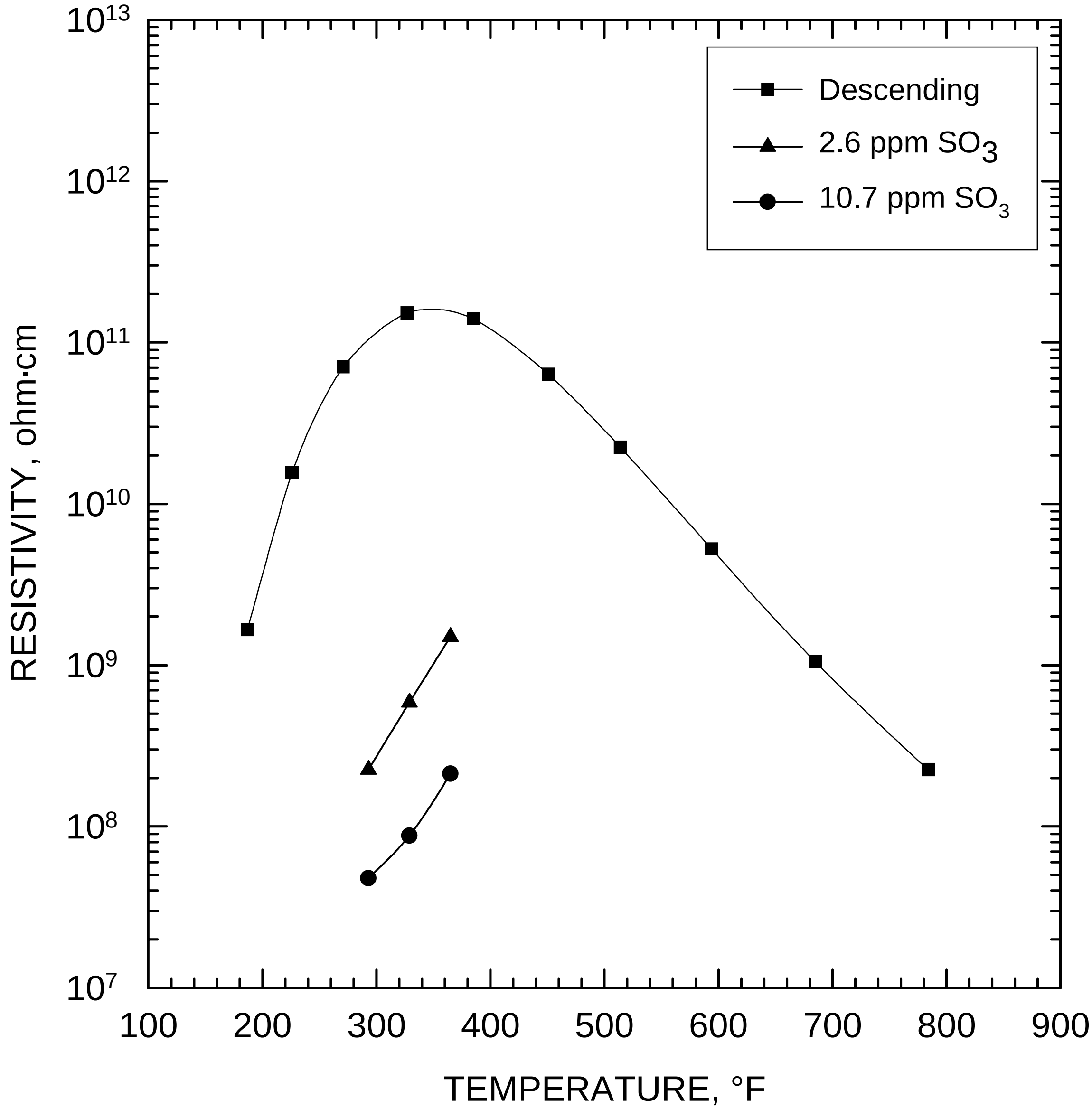

Figure B-13. Laboratory resistivity of Sample 9896-1-124 with 10.2 % water by volume and two SO_3 injection rates at specific temperatures.

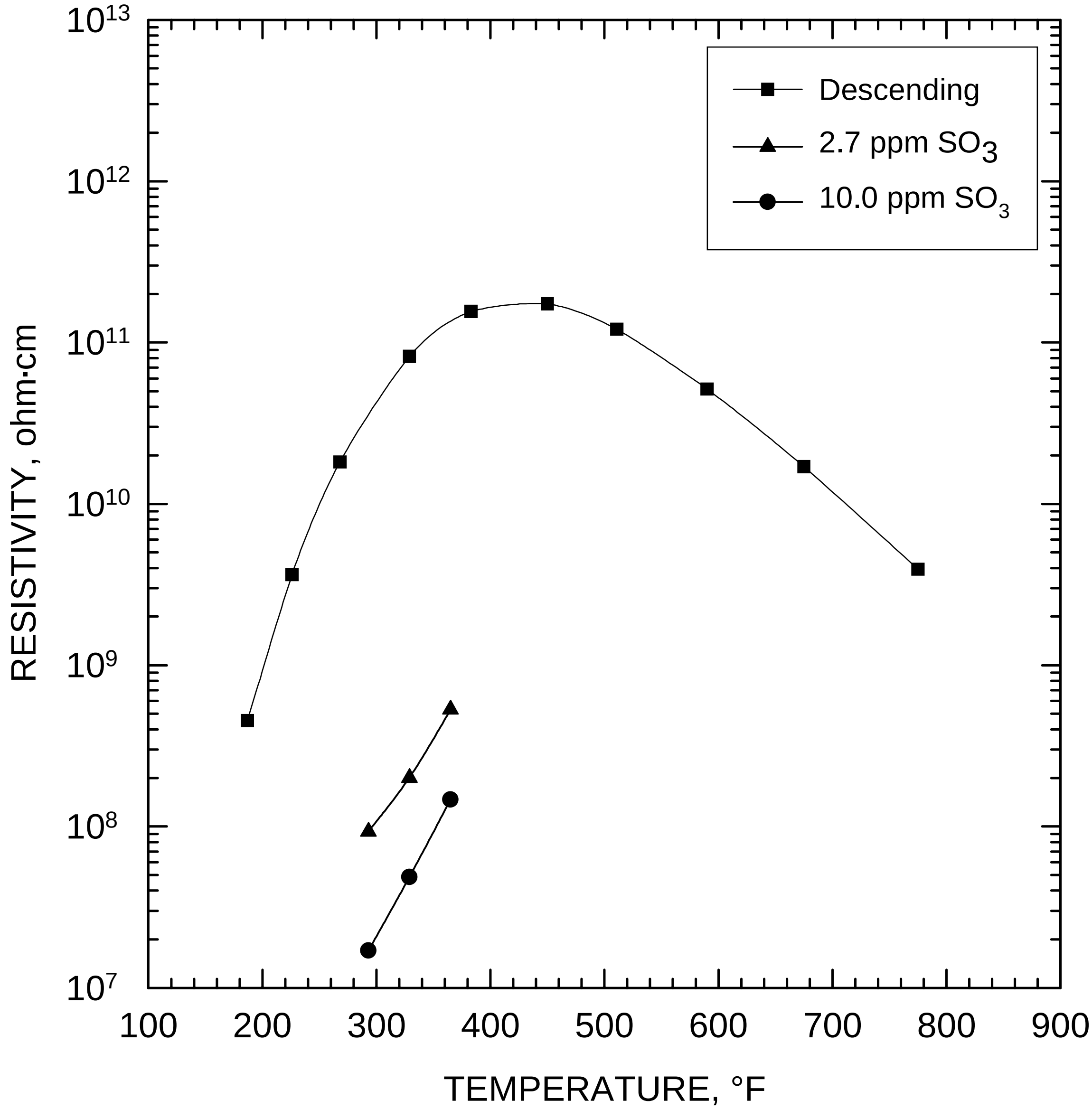

Figure B-14. Laboratory resistivity of Sample 9896-1-130 with 10.0 % water by volume and two SO_3 injection rates at specific temperatures.

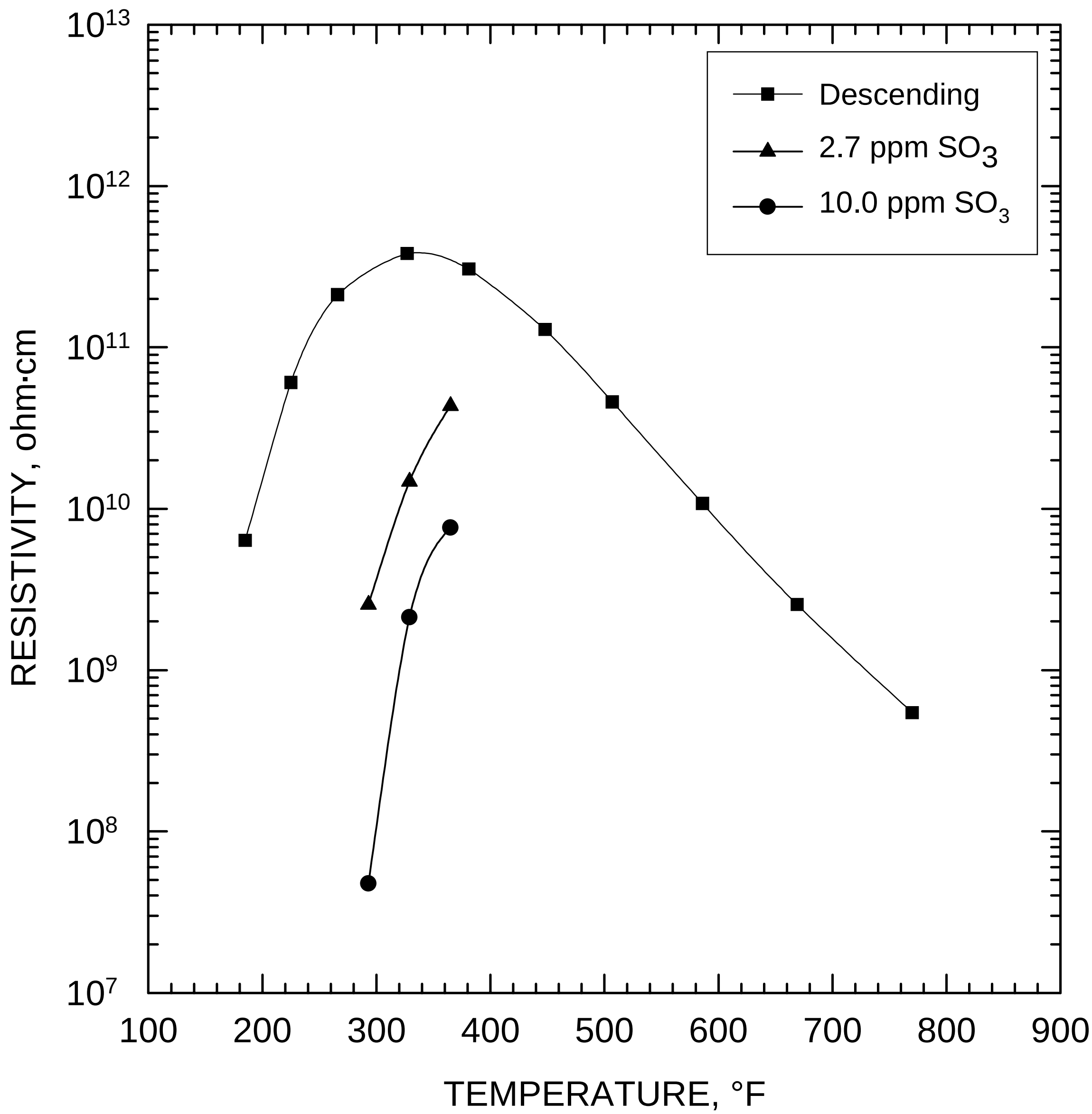

Figure B-15. Laboratory resistivity of Sample 9896-1-133 with 10.0 % water by volume and two SO_3 injection rates at specific temperatures.

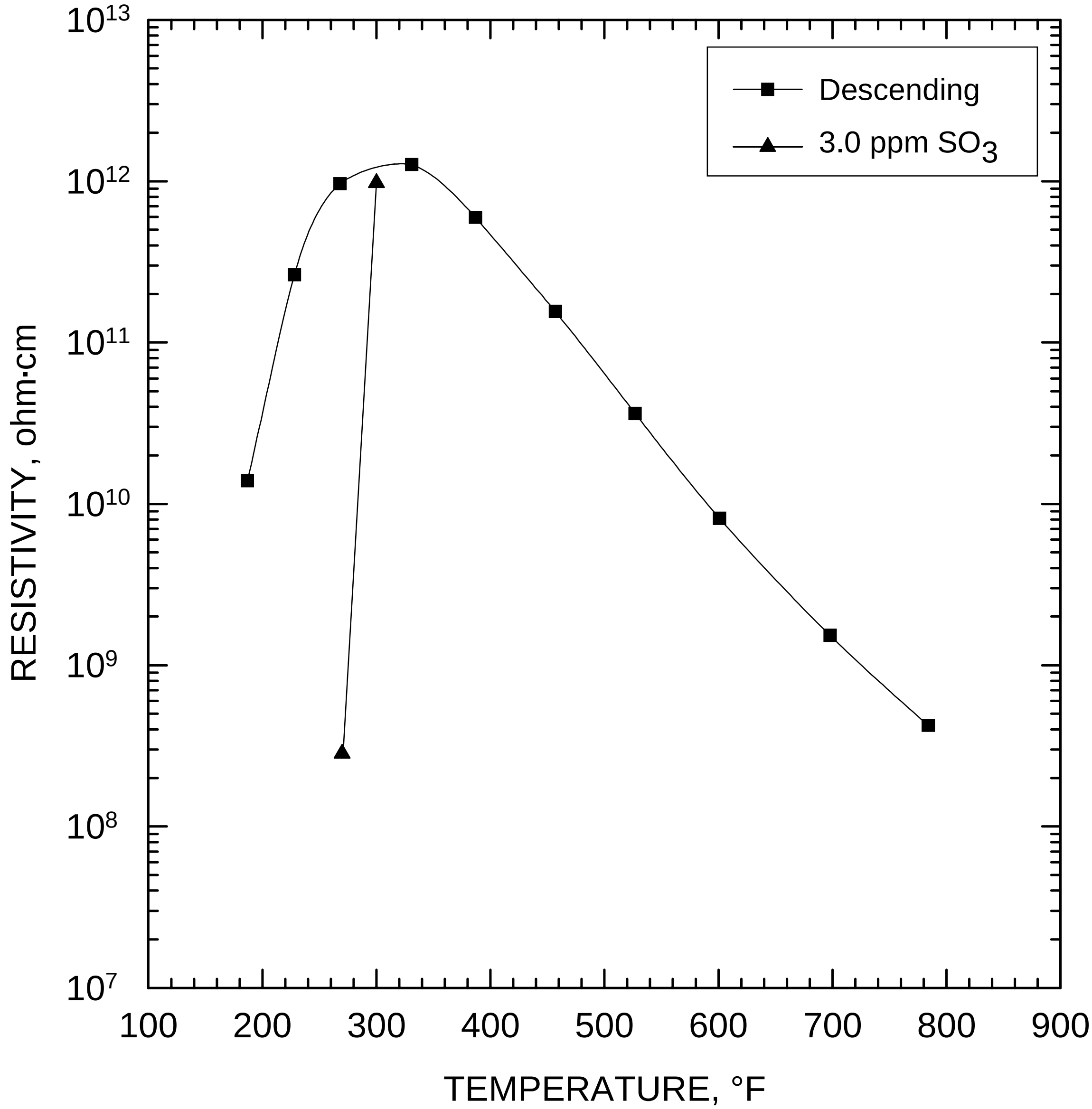

Figure B-16. Laboratory resistivity of Sample D492A with 10.4 % water by volume and one SO_3 injection rate at specific temperatures.

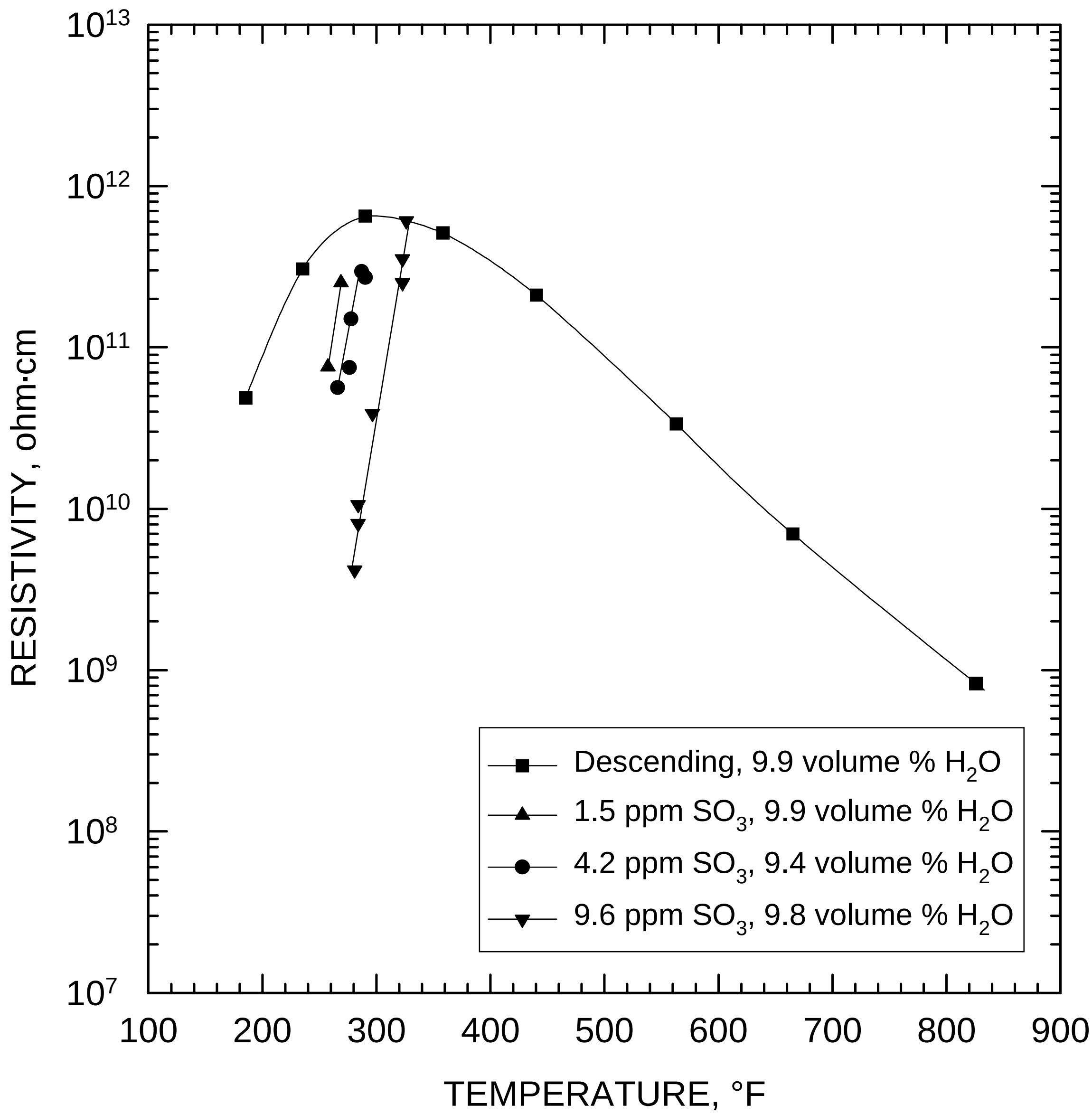

Figure B-17. Laboratory resistivity of Sample 301 with three SO_3 injection rates at specific temperatures.

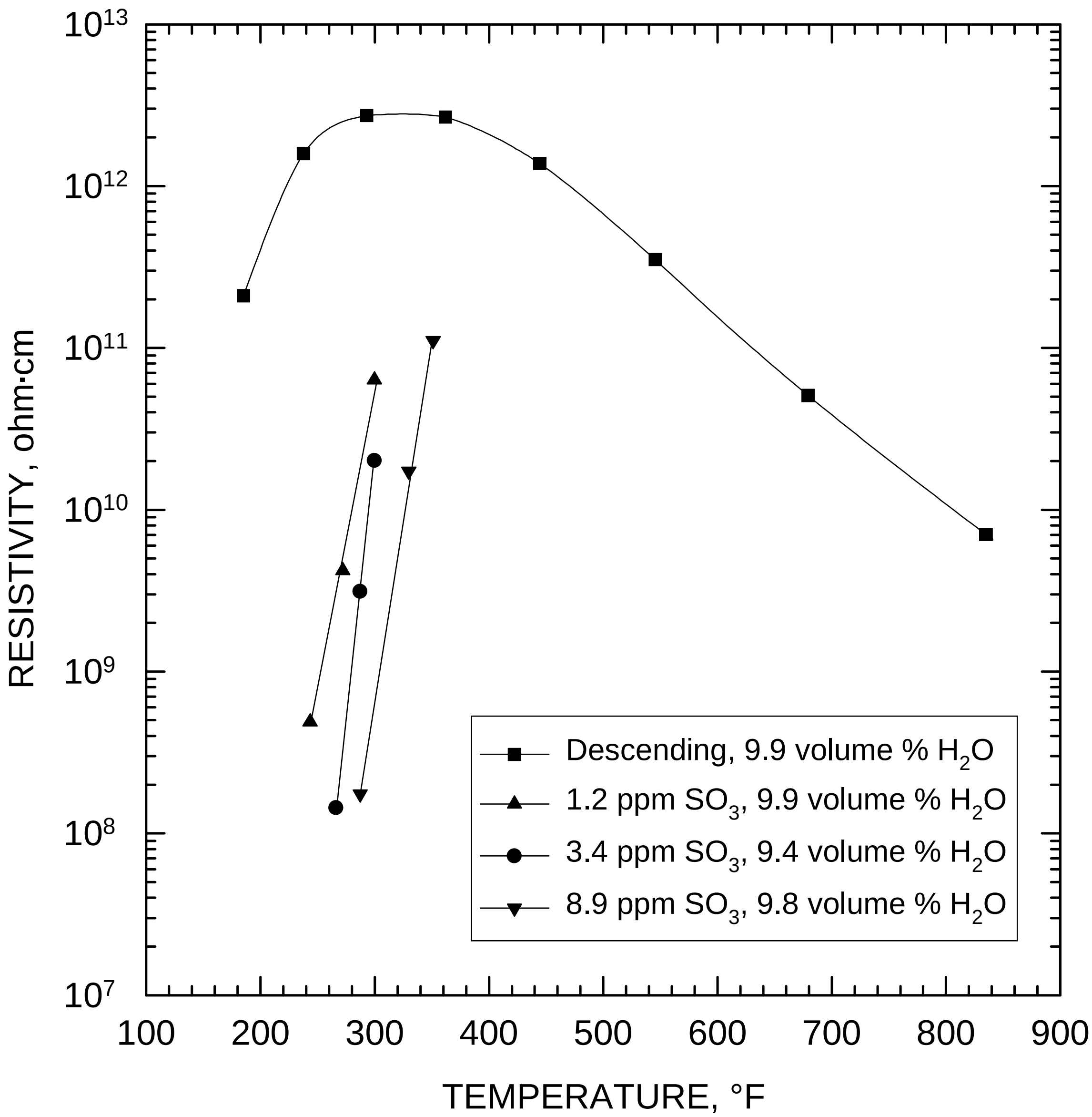

Figure B-18. Laboratory resistivity of Sample 302 with three SO_3 injection rates at specific temperatures.

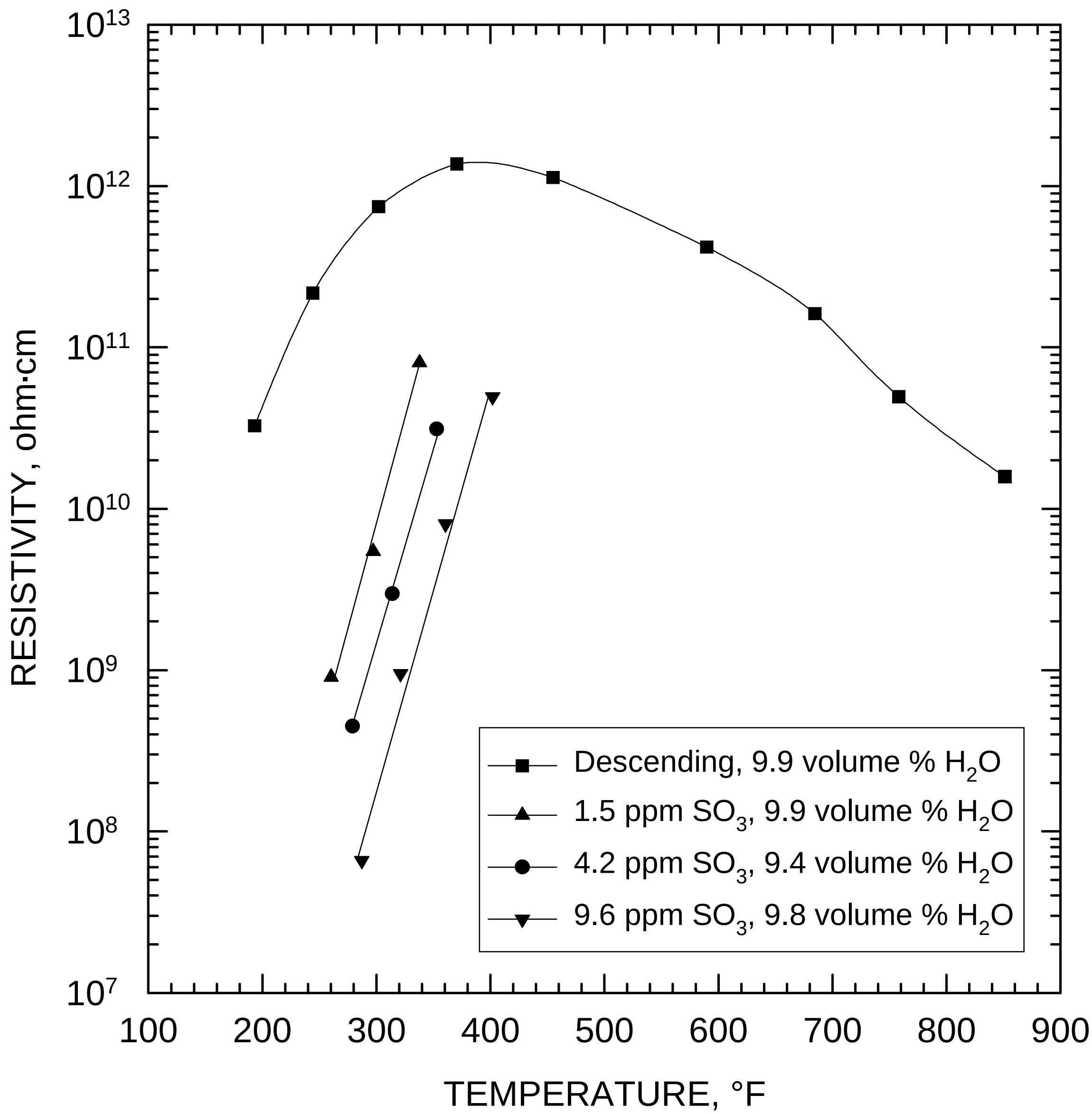

Figure B-19. Laboratory resistivity of Sample 303 with three SO_3 injection rates at specific temperatures.

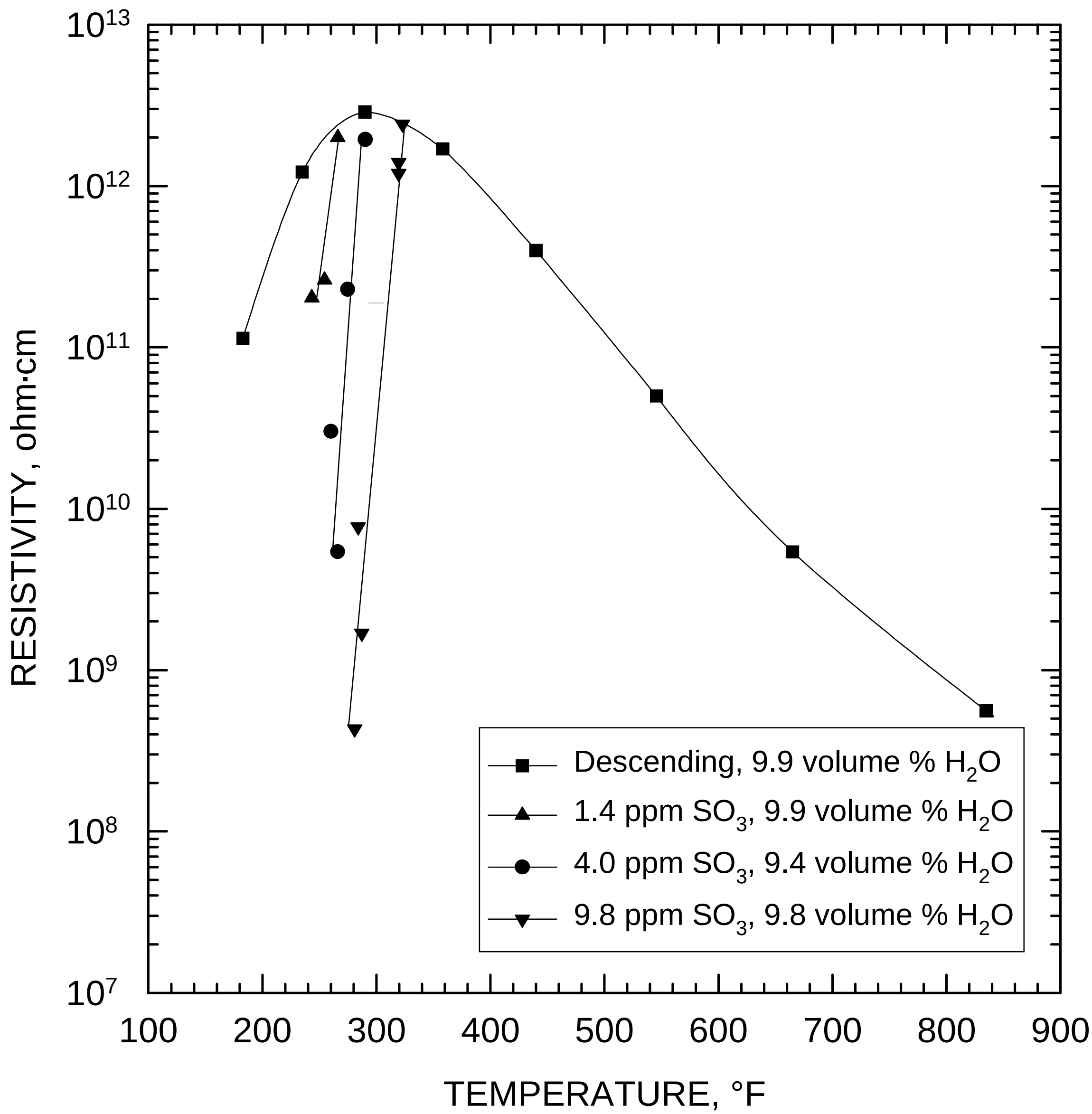

Figure B-20. Laboratory resistivity of Sample 304 with three SO_3 injection rates at specific temperatures.

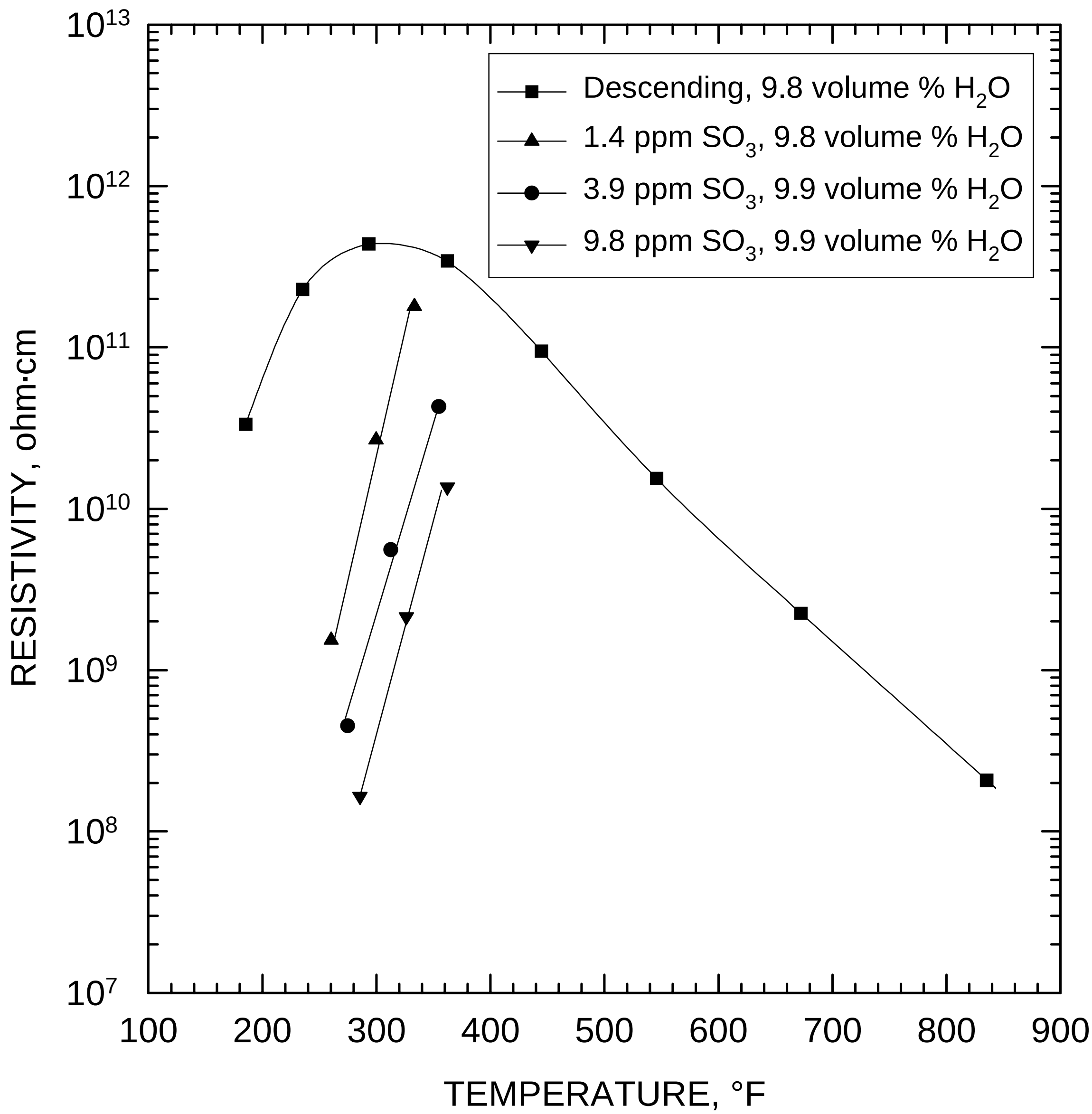

Figure B-21. Laboratory resistivity of Sample 305 with three SO_3 injection rates at specific temperatures.

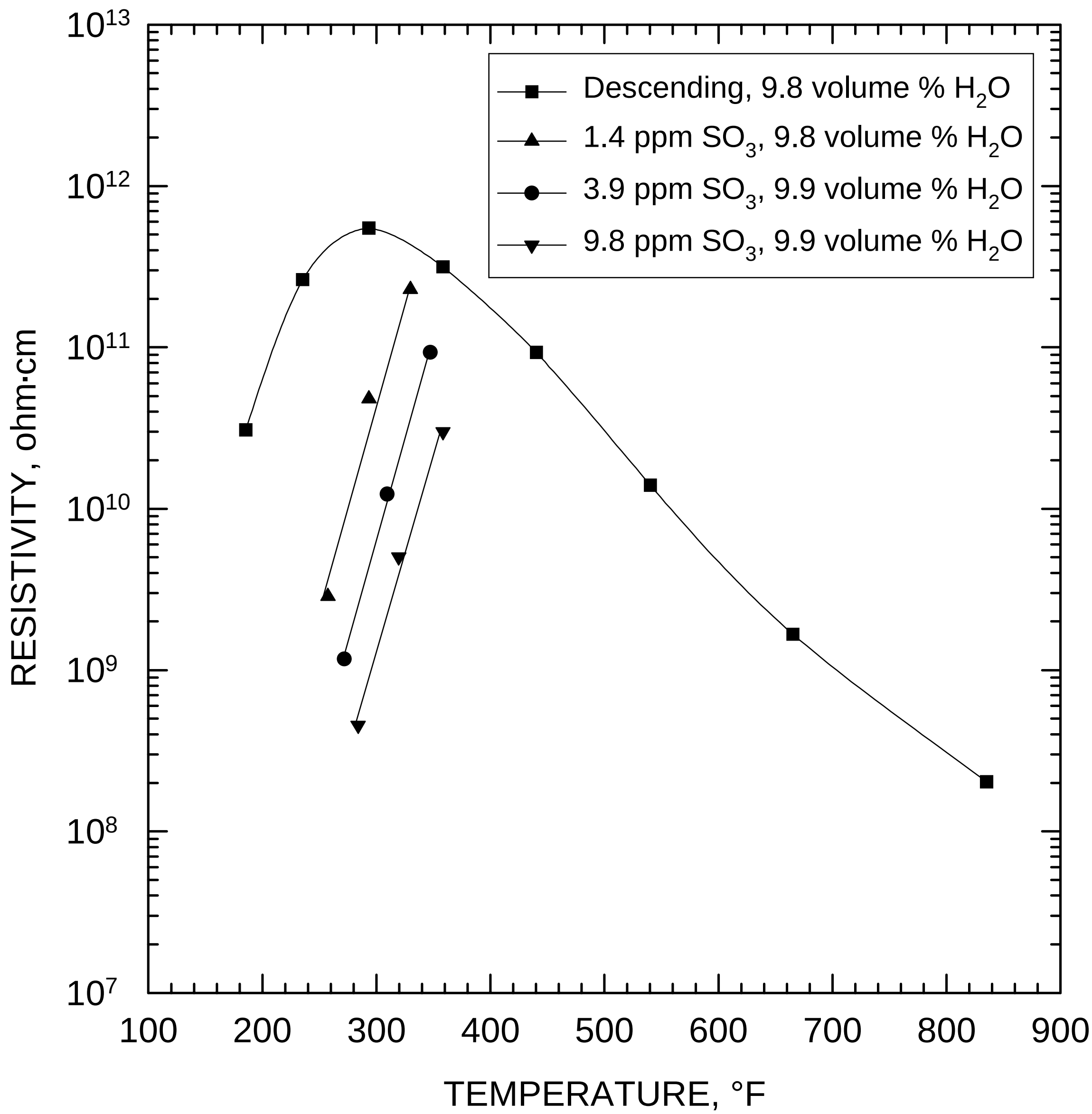

Figure B-22. Laboratory resistivity of Sample 306 with three SO_3 injection rates at specific temperatures.

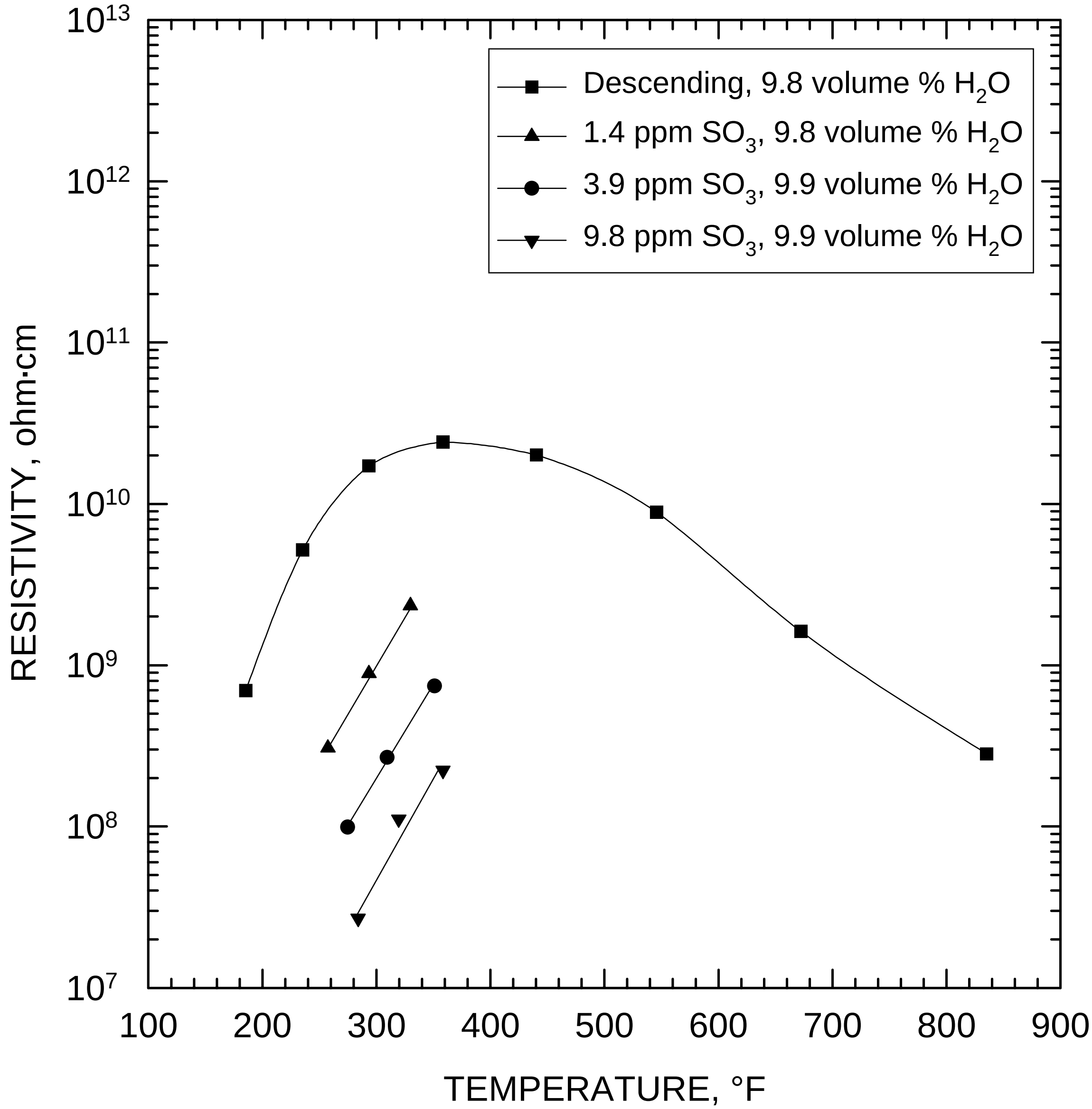

Figure B-23. Laboratory resistivity of Sample 307 with three SO_3 injection rates at specific temperatures.

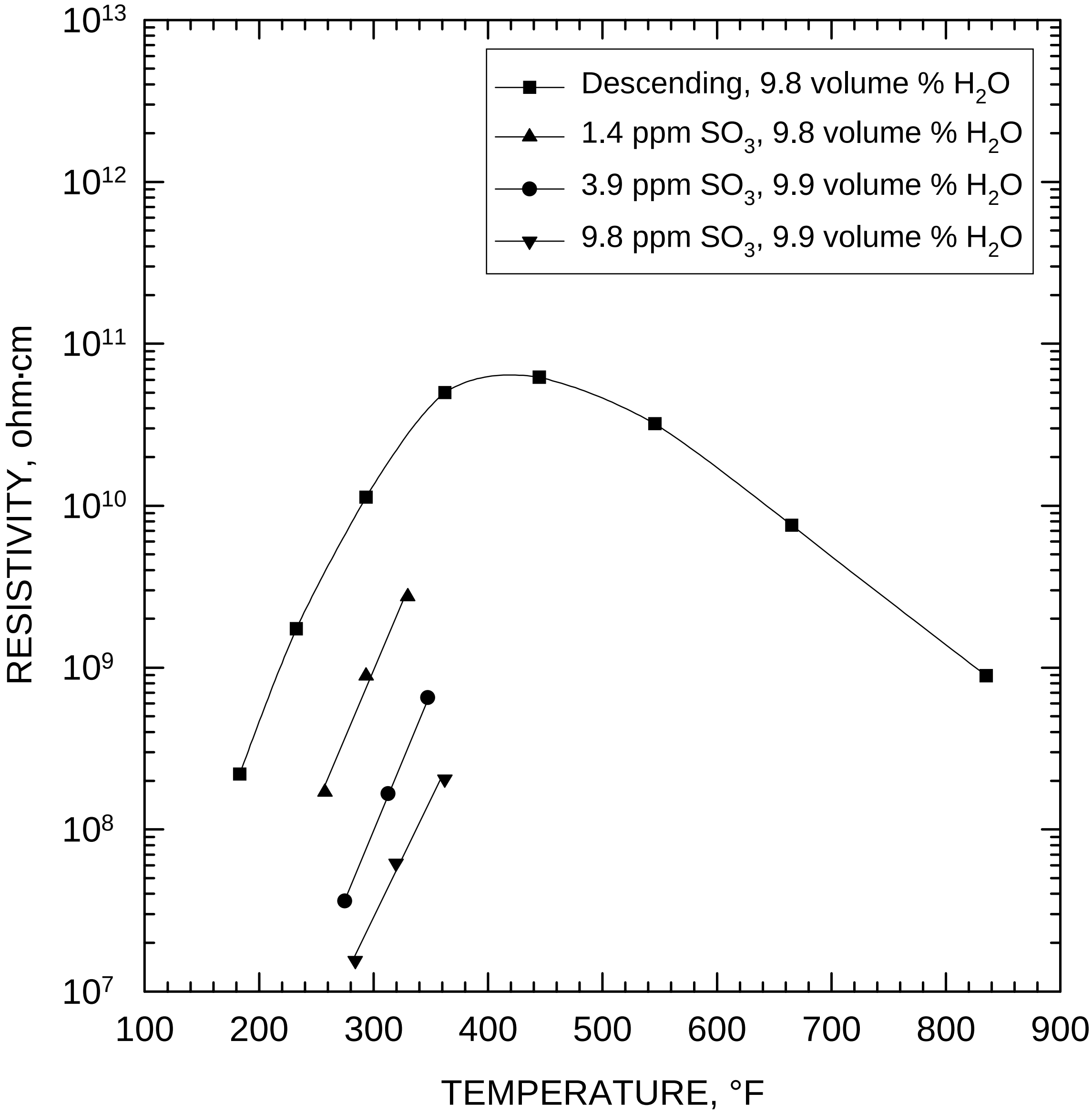

Figure B-24. Laboratory resistivity of Sample 308 with three SO_3 injection rates at specific temperatures.

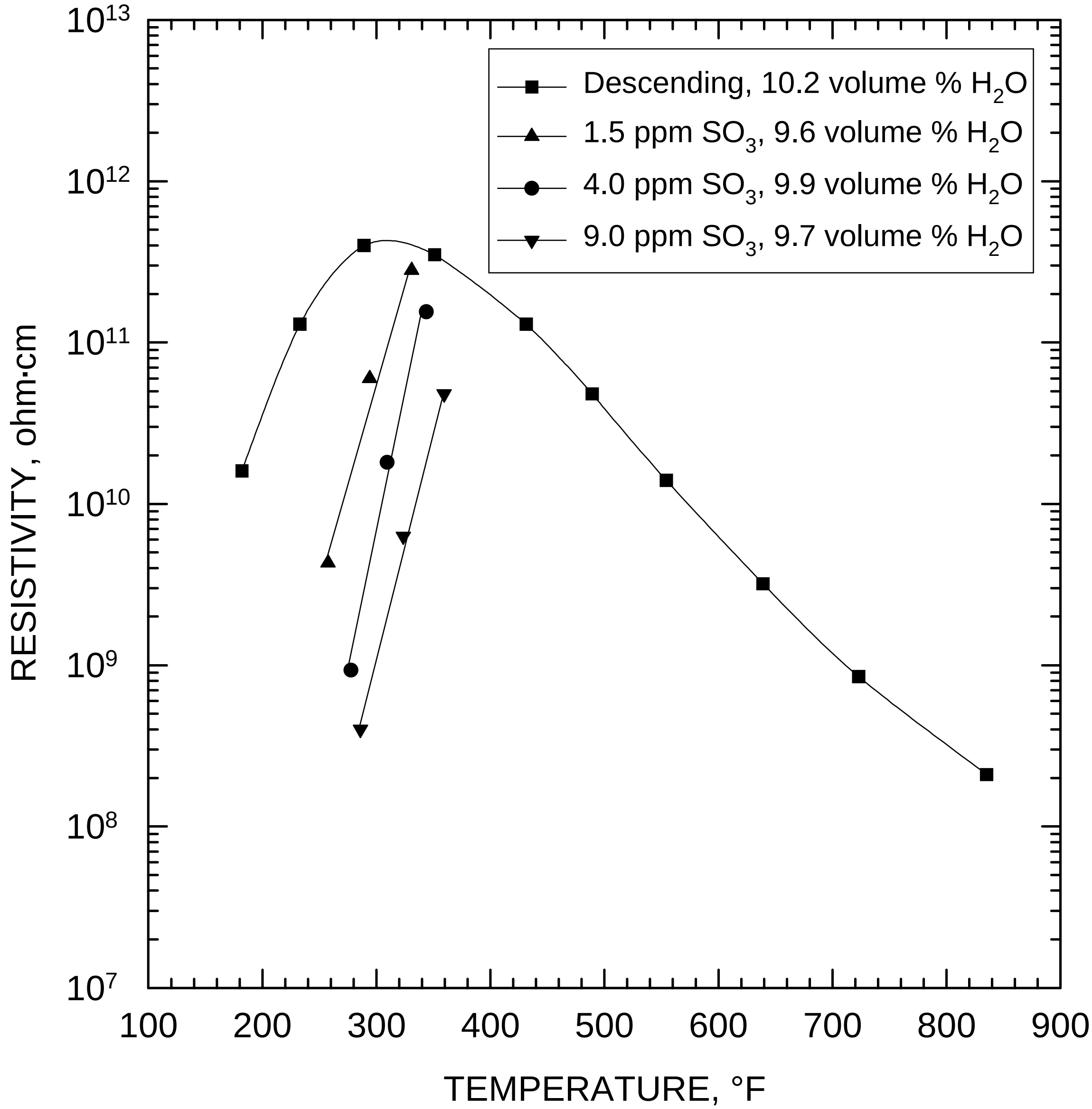

Figure B-25. Laboratory resistivity of Sample 311 with three SO_3 injection rates at specific temperatures.

About EPRI

EPRI creates science and technology solutions for the global energy and energy services industry. U.S. electric utilities established the Electric Power Research Institute in 1973 as a nonprofit research consortium for the benefit of utility members, their customers, and society. Now known simply as EPRI, the company provides a wide range of innovative products and services to more than 1000 energy-related organizations in 40 countries. EPRI's multidisciplinary team of scientists and engineers draws on a worldwide network of technical and business expertise to help solve today's toughest energy and environmental problems.

EPRI. Electrify the World

Printed on recycled paper in the United States of America

1000657

SINGLE USER LICENSE AGREEMENT

THIS IS A LEGALLY BINDING AGREEMENT BETWEEN YOU AND THE ELECTRIC POWER RESEARCH INSTITUTE, INC. (EPRI). PLEASE READ IT CAREFULLY REMOVING THE WRAPPING MATERIAL.

BY OPENING THIS SEALED PACKAGE YOU ARE AGREEING TO THE TERMS OF THIS AGREEMENT. IF YOU DO NOT AGREE TO THE TERMS OF THIS AGREEMENT, PROMPTLY RETURN THE UNOPENED PACKAGE TO EPRI AND THE PURCHASE PRICE WILL BE REFUNDED.

1. GRANT OF LICENSE

EPRI grants you the nonexclusive and nontransferable right during the term of this agreement to use this package only for your own benefit and the benefit of your organization. This means that the following may use this package: (I) your company (at any site owned or operated by your company); (II) its subsidiaries or other related entities; and (III) a consultant to your company or related entities, if the consultant has entered into a contract agreeing not to disclose the package outside of its organization or to use the package for its own benefit or the benefit of any party other than your company.

This shrink-wrap license agreement is subordinate to the terms of the Master Utility License Agreement between most U.S. EPRI member utilities and EPRI. Any EPRI member utility that does not have a Master Utility License Agreement may get one on request.

2. COPYRIGHT

This package, including the information contained in it, is either licensed to EPRI or owned by EPRI and is protected by United States and international copyright laws. You may not, without the prior written permission of EPRI, reproduce, translate or modify this package, in any form, in whole or in part, or prepare any derivative work based on this package.

3. RESTRICTIONS

You may not rent, lease, license, disclose or give this package to any person or organization, or use the information contained in this package, for the benefit of any third party or for any purpose other than as specified above unless such use is with the prior written permission of EPRI. You agree to take all reasonable steps to prevent unauthorized disclosure or use of this package. Except as specified above, this agreement does not grant you any right to patents, copyrights, trade secrets, trade names, trademarks or any other intellectual property, rights or licenses in respect of this package.

4. TERM AND TERMINATION

This license and this agreement are effective until terminated. You may terminate them at any time by destroying this package. EPRI has the right to terminate the license and this agreement immediately if you fail to comply with any term or condition of this agreement. Upon any termination you may destroy this package, but all obligations of nondisclosure will remain in effect.

5. DISCLAIMER OF WARRANTIES AND LIMITATION OF LIABILITIES

NEITHER EPRI, ANY MEMBER OF EPRI, ANY COSPONSOR, NOR ANY PERSON OR ORGANIZATION ACTING ON BEHALF OF ANY OF THEM:

(A) MAKES ANY WARRANTY OR REPRESENTATION WHATSOEVER, EXPRESS OR IMPLIED, (I) WITH RESPECT TO THE USE OF ANY INFORMATION, APPARATUS, METHOD, PROCESS OR SIMILAR ITEM DISCLOSED IN THIS PACKAGE, INCLUDING MERCHANTABILITY AND FITNESS FOR A PARTICULAR PURPOSE, OR (II) THAT SUCH USE DOES NOT INFRINGE ON OR INTERFERE WITH PRIVATELY OWNED RIGHTS, INCLUDING ANY PARTY'S INTELLECTUAL PROPERTY, OR (III) THAT THIS PACKAGE IS SUITABLE TO ANY PARTICULAR USER'S CIRCUMSTANCE; OR

B) ASSUMES RESPONSIBILITY FOR ANY DAMAGES OR OTHER LIABILITY WHATSOEVER (INCLUDING ANY CONSEQUENTIAL DAMAGES, EVEN IF EPRI OR ANY EPRI REPRESENTATIVE HAS BEEN ADVISED OF THE POSSIBILITY OF SUCH DAMAGES) RESULTING FROM YOUR SELECTION OR USE OF THIS PACKAGE OR ANY INFORMATION, APPARATUS, METHOD, PROCESS OR SIMILAR ITEM DISCLOSED IN THIS PACKAGE.

6. EXPORT

The laws and regulations of the United States restrict the export and re-export of any portion of this package, and you agree not to export or re-export this package or any related technical data in any form without the appropriate United States and foreign government approvals.

7. CHOICE OF LAW

This agreement will be governed by the laws of the State of California as applied to transactions taking place entirely in California between California residents.

8. INTEGRATION

You have read and understand this agreement, and acknowledge that it is the final, complete and exclusive agreement between you and EPRI concerning its subject matter, superseding any prior related understanding or agreement. No waiver, variation or different terms of this agreement will be enforceable against EPRI unless EPRI gives its prior written consent, signed by an officer of EPRI.

EPRI • 3412 Hillview Avenue, Palo Alto, California 94304 • PO Box 10412, Palo Alto, California 94303 • USA
800.313.3774 • 650.855.2121 • askepri@epri.com • www.epri.com